DOE/PC/90160--T4

DE92 016806

ADVANCED ATOMIZATION CONCEPT FOR CWF BURNING IN SMALL COMBUSTORS - PHASE II

Final Technical Report

Contract No. DE-AC22-90PC90160

Edward T. McHale
Harley L. Heaton

Technology Department
Atlantic Research Corporation
5945 Wellington Road
Gainesville, VA 22065

Submitted to:

U.S. Department of Energy
Pittsburgh Energy Technology Center
P.O. Box 10940, MS 922-H
Pittsburgh, PA 15236

Attention: Mr. Anthony Mayne, Project Manager

ARC No. 38-5392

December 1991

TABLE OF CONTENTS

LIST OF ILLUSTRATIONS

LIST OF TABLES

1.0 INTRODUCTION AND SUMMARY

The program described in this report represents a continuation of an earlier study that proposed and verified a concept referred to as opposed-jet atomization, which is particularly applicable to coal-water fuel (CWF). The Final Technical Report of that study was dated September 1989 and was conducted under Department of Energy Contract No. DE-AC22-87PC79656 ("Advanced Atomization Concept for CWF Burning in Small Combustors," E. T. McHale, H. L. Heaton, and J. H. Lippold, Atlantic Research Corporation No. 38-5268). Results were also published in the Proceedings of the Fourteenth International Conference on Coal and Slurry Technology, April 1989, Coal and Slurry Technology Association, Washington, D.C. A brief summary of results of the earlier program will be given here; however, readers may want to refer to the original reports if details are required.

Most atomizer designs employ either a stream of fuel that is impacted internally by an air blast to produce a spray; or a jet of fuel that issues from an orifice and externally encounters an annular flow of air, causing atomization by parallel shear. In the present atomizer design, two opposed jets of CWF are directed at each other and externally encounter a perpendicular blast of air at the collision point to create a spray of much finer droplets. This is shown schematically below.

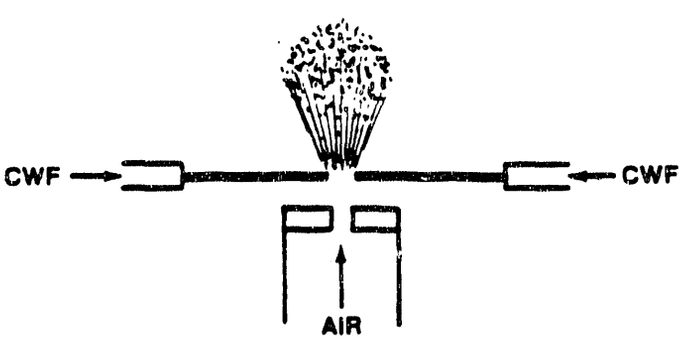

Schematic of Opposed-Jet Atomization Concept

This opposed-jet concept has been shown to produce sprays with CWF of mass median diameters (MMD) in the 20-micron range at atomizing air-to-fuel (A/F) ratios of about 0.5. The earlier work was conducted at a capacity

equivalent to approximately 1 MMBTU/H. The present study extended this down to 0.24 MMBTU/H and to as high as 4.3 MMBTU/H (the upper limit being set by equipment limitations). Only cold-flow testing was performed in the present effort; combustion tests are to be conducted at the U.S. Department of Energy (DOE), Pittsburgh Energy Technology Center (PETC), the sponsor of the program.

In the earlier Phase I program, both cold flow and combustion testing were performed. A number of atomizer parameters were evaluated and optimized in the cold-flow tests, including the distance between the CWF jets, the distance between the collision zone and the atomizing air orifice, the relative sizes of the CWF and air orifices for a capacity of 1 MMBTU/H, and the atomizing A/F ratio. After having completed this cold-flow testing with a prototype test unit, an operational atomizer was designed and fabricated for use in the Atlantic Research 1 MMBTU/H experimental furnace. The combustion phase of the work involved measuring CWF combustion efficiency for a range of operating parameters, including CWF flow rate, atomizer air pressure and flow rate, secondary air preheat, CWF preheat, secondary air swirl strength; and also CWF properties that affect atomizer performance, such as solids content, viscosity, and particle size distribution. Combustion efficiencies with the opposed-jet atomizer ran in the range of 96%, with some values of 97 and 98%. They depend among other things on the coal type. These were considered excellent for the test furnace being used, since in an earlier program the best that could be obtained with a different atomizer were values in the high 80 percent range.

The present Phase II program involved further evaluation of the opposed-jet atomizer performance plus a number of associated tasks. The latter included an erosion study of CWF orifices made of several materials, and also the production of over 2000 gallons of CWF fuels for use by PETC in the Fuel Evaluation Facility (FEF) of 0.5 MMBTU/H capacity. In addition, an atomizer was fabricated and tested for PETC use in the FEF. The atomizer performance tasks included the testing of slotted air jets in place of circular orifices, acquisition and testing of an alternative atomizer (a Parker Hannifin unit) for comparative purposes, testing of CWF's covering a range of viscosities, and a study of the scaling of the atomizer to lower and higher capacities than the 0.5 MMBTU/H target.

The scaling study was especially revealing. It was found that the opposed-jet atomizer showed better performance when it was scaled-up to 4.3 MMBTU/H, relative to 1 MMBTU/H; however, the performance, as judged by droplet size, was poorer as the atomizer was scaled-down to 0.24 MMBTU/H. With all the experimental results available, extending well over an order of magnitude in capacity, it was possible to formulate and verify a quantitative model that explains the operation of the atomizer and which allows prediction of the operating parameters required for optimum performance. These parameters, which must achieve certain minimum values, are A/F ratio, atomizing air blast force, and ratio of force of CWF jets to that of atomizing air.

2.0 EXPERIMENTAL CALIBRATIONS AND FUEL DATA

The experimental testing was performed using an opposed-jet prototype atomizer unit very similar to that previously used in Phase I. Atomizing air was provided by an air compressor which could deliver up to about 30 g/sec (240 lb/hr) at a pressure of about 90 psia; however, this level could not consistently be sustained, and often a limit of about 25 g/sec at 80 psia was imposed by the compressor. At lower mass rates, higher pressures could be attained.

CWF was delivered through a system consisting of a Moyno pump and two basket screen filters (70 mesh) arranged in parallel with the injectors. Driving pressures were variable depending on the flow rate, orifice diameter, and cleanliness of the filters.

Spray droplet sizes were measured with a Malvern Model 2200/3300 particle size analyzer equipped with a 300 mm focal length lens. Tubular extensions on the laser source unit and detector unit were used through which air flowed in order to prevent spray from contaminating the optics. The laser beam passed through the CWF spray about four inches from the atomizer source. Tests at three and five inches showed no difference in spray droplet size.

One experimental problem was encountered because of the nature of the atomizer type. When the atomizing air blast hits the CWF jets, two spray "lobes" form downstream for a short distance (but greater than five inches before they merge), one above and one below the jet flows. This behavior resembles an air blast hitting a solid rod with the air having to flow above and below it to get by. No operational problems, such as in a combustor firing, would be caused by this behavior; however, in determining a spray droplet size distribution, it was important to center the laser beam in the middle of one of the lobes. The testing problem that this gives rise to is that as atomization pressure is increased, the size of the lobes decrease and the laser beam may shine through an off-center position. Special care was taken to minimize this problem, but some of the reproducibility of the data is limited by this.

2.1 Calibration of Test System

The Malvern particle size analyzer was calibrated for accuracy and reproducibility using standard glass beads available for calibration purposes from the National Institute of Standards and Technology (NIST). The calibration against NIST standard beads of 5-30 microns diameter is shown in Figure 1. The points represent five separate tests. Overall, the data reproduce the standard NIST curve on the figure very well; however, the scatter is appreciably greater than the error bands on the S-curve. We attribute the scatter to the fact that the Malvern particle size analyzer is set up to measure spray droplets, and the calibration must be performed with the NIST standard glass beads in a water suspension. Accordingly, the liquid analyzer cell had to be hand-held in the path of the laser beam during the calibration testing, giving rise to irreproducibility. For this reason, we did five separate tests and plotted all the data together. We feel confident that the absolute accuracy of the instrument is completely satisfactory, as is the reproducibility of measurements in sprays as shown by the data below.

Two series of "reproducibility" tests were performed with water sprays. The first employed a set of (brass) orifices for the water jet that had previously been used quite extensively, to the point that the orifice diameters had increased from 0.024" to slightly greater than 0.025" (about a 10% area increase). The streams of water that issued from the orifices were visually irregular and would change slightly during a test. The data were taken by running a set of five tests at pressures of 40, 70, 100, 70, 40 psig, then shutting the system down for a while, restarting and repeating, for a total of five sets of five tests each. The results are collected in Table 1, listed as mass median diameter of each spray (Sauter mean diameters would be slightly lower).

The data are reasonably reproducible with an overall average [(standard deviation/average MMD) x 100] of 14%. This result can be compared with the comparable value of about 22% reported in Phase I of the program (2nd Quarterly Report, November 1987 - January 1988, Contract No. DE-AC22-87PC79656).

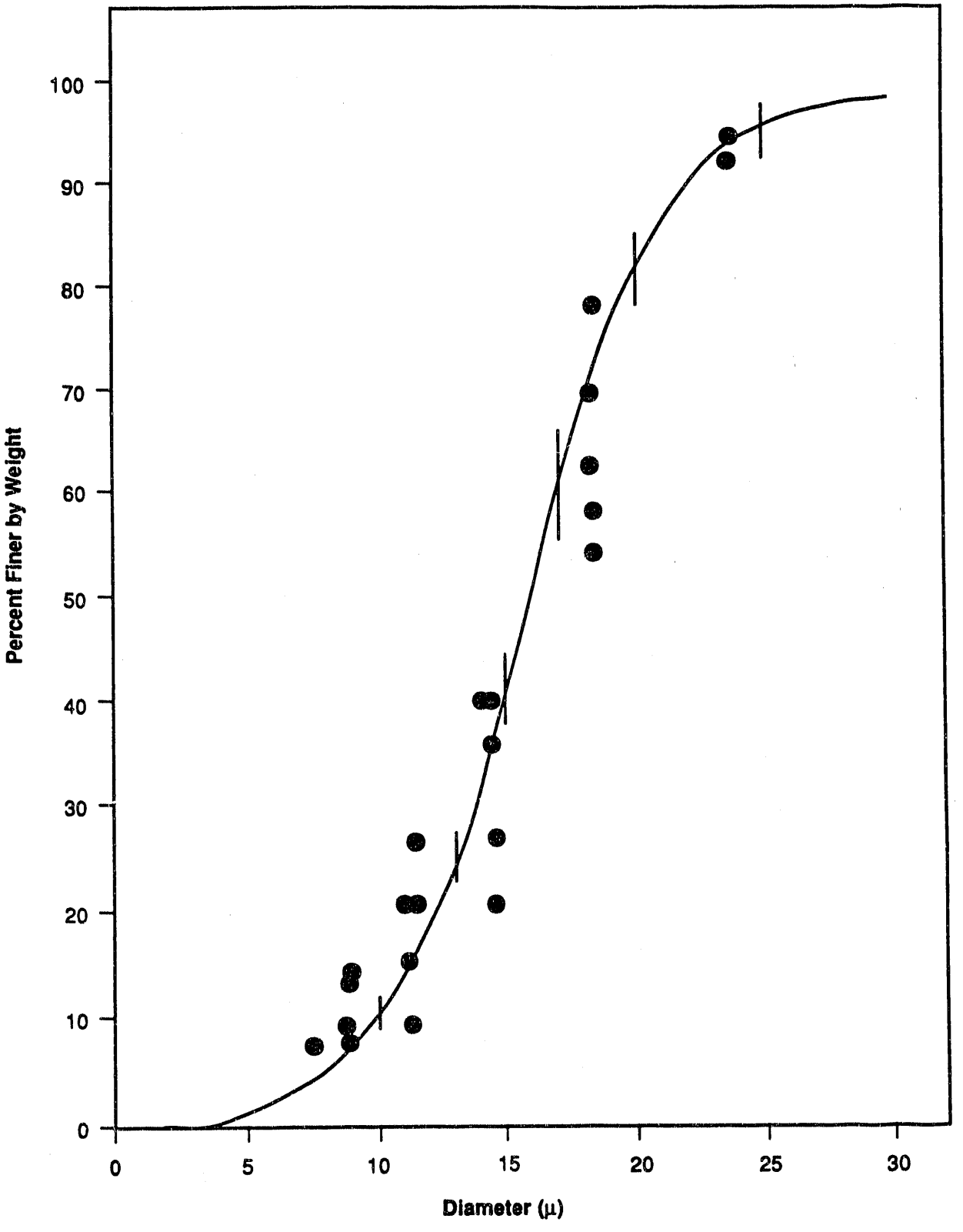

Figure 1

Malvern Calibration Test Results. ARC Data (Points) Versus NIST Standard Glass Beads (S-Curve)

Table 1. Reproducibility Test Results Using Water Sprays and Eroded Orifices

Water Orifice Diameters	- 0.025"
Water Flow Rate	- 22.1 g/sec
Air Orifice Diameter	- 0.125"
Distance From Spray Collision Zone to Laser Beam	- 4"
Distance from Air Orifice to Collision Zone	- 12 mm
Distance Between Water Nozzle Orifices	- 2"

Pressure (psia)	55.0	85.0	115.0	85.0	55.0
$\dot{m}$ (air) (g/sec)	5.2	8.0	10.8	8.0	5.2
A/F Ratio	0.24	0.36	0.49	0.36	0.24
Mass Median Droplet Diameter (microns)	30	18	10.4	17	29
	24	13	7.8	13	24
	31	17	11.6	17	30
	30	17	10.4	19	36
	33	20	11.6	19	34
Average MMD's	30.0	17.0	10.4	17.0	31.0
Standard Deviation	3.4	2.5	1.6	2.4	4.7
Standard Deviation/Average x 100 (%)	11.0	15.0	15.0	14.0	15.0

In an effort to try to improve on the reproducibility, the old nozzles were replaced with new nozzles of 0.020" diameter. The appearance of the water streams was markedly improved; and as can be seen from the data listed in Table 2, the reproducibility is much better, with an overall average [(standard diameter/average MMD) x 100] of 6%. It is noted that the MMD's of these sprays are higher (at the higher atomizing pressures) than those of the sprays from the 0.025" orifice of Table 1. This is attributed to the fact that at the smaller orifice diameter, the driving force per unit area of the H_2O jets was lower than with the larger orifices. As the orifice diameter decreased from 0.025" to 0.020", a 36% decrease in area, the flow rate decreased from 22.1 g/sec to 10.5 g/sec, or 52.5% at the same driving pressure. (This disproportionate drop in flow rate is attributed in turn to a lower discharge coefficient for the smaller liquid orifice.) However, this disproportionate drop led to a relatively weaker H_2O jet that could not adequately penetrate the air blast. This phenomenon is discussed at length in Section 4.0 on Analysis of Opposed-Jet Atomization Process.

Table 2. Reproducibility Test Results Using Water Sprays and New Orifices

Water Orifice Diameters	- 0.020"
Water Flow Rate	- 10.5 g/sec
Air Orifice Diameter	- 0.125"
Distance From Spray Collision Zone to Laser Beam	- 4"
Distance from Air Orifice to Collision Zone	- 12 mm
Distance Between Water Nozzle Orifices	- 2"

Pressure (psia)	40.0	50.0	60.0	50.0	40.0
$\dot{m}$ (air) (g/sec)	3.8	4.7	5.6	4.7	3.8
A/F Ratio	0.36	0.45	0.54	0.45	0.36
Mass Median Droplet Diameter (microns)	28	21	18	23	32
	33	23	19	25	31
	32	24	18	25	34
	34	26	19	25	35
Average MMD's	32.0	24.0	18.5	25.0	33.0
Standard Deviation	2.6	2.2	0.6	1.2	1.8
Standard Deviation/Average x 100 (%)	8.0	9.0	3.0	5.0	5.0

2.2 Measurement of Mass Flow of CWF and Atomization Air

In the case of the CWF slurries, the measurement of mass flow rates was straightforward and was performed for each atomization test. CWF was pumped by a positive displacement Moyno pump through basket-type screen filters of 70 mesh in line with the orifices. A reservoir container (five gallons) of CWF was positioned on an analytical balance of 20-kilogram capacity and one-gram sensitivity. During each test, a flow rate was established through a set of CWF orifices, and then loss in weight of the container was measured over a given period of time to give $\dot{m}_F$ directly.

In the case of atomizing air, the mass flow was calculated from the gas dynamic discharge equation for flow through a critical (choked) orifice:

$$\dot{m} = CAP\sqrt{\frac{\gamma M}{RT}}\,(0.58)\ g/sec$$

With A = Orifice Area (cm^2)

P = $\frac{psia}{14.7} \times 10^6$ dynes/cm^2 (referred to as upstream pressure, P_u, later)

γ = Heat capacity ratio = 1.4 for air

R = Gas constant = 8.3×10^7 cgs units

T = 300°K

The factor 0.58 represents the so-called thermodynamic efficiency factor and is given by:

$$(2/(\gamma + 1))^{\frac{\gamma + 1}{2(\gamma - 1)}}$$

The discharge coefficient, C (referred to later as C_D), must be experimentally measured for each orifice. This was accomplished by measuring the flow rate of water through the orifices, which represents a standard method for obtaining C and is sufficiently accurate for purposes of the present study. (Reference: Measurement Systems, E. O. Doebelin, McGraw-Hill, 1975.) The requirement of this method is that the pertinent similarity relation, the Reynolds number, be maintained. The N_{Re} for the atomizing air orifices is given by:

$$N_{Re} = \frac{\rho v d}{\mu} = \frac{(\dot{m}/A)d}{\mu} = \frac{4\dot{m}}{\pi d \mu}$$

where A and d are the orifice area and diameter, and μ is the viscosity of air, taken as 1.85×10^{-4} poise. Values for various orifices and conditions are:

Orifice Diameter		$\dot{m}_{air}$	
(inch)	(cm)	(g/sec)	N_{Re}
1/16	0.159	0.7	3.0×10^4
1/8	0.318	8.0	1.7×10^5
1/4	0.635	32.0	3.5×10^5

These represent the extremes of the parameters of the table. As will be seen from the test data, the range of N_{Re} values is the important condition. Actually, in order to calculate the values for $\dot{m}_{air}$, the C_d values must be known or estimated. The values listed later were used here.

The procedure to obtain C_D values for the air orifices is to drive water at a known pressure through the orifices (positioned exactly in their retaining fittings as when used with air), to measure the mass flow rate of the water by collecting and weighing over a known time, and then to compare these actual rates with the theoretically-calculated rates and, thus, derive C_D values. As mentioned, the testing must be at the same Reynolds number. The theoretical mass flow of water is:

$$\dot{m}_{H_2O} = C_D \, A\rho v$$

and since $P = 1/2 \, \rho v^2$

$$\dot{m}_{H_2O} = C_D \, A \, \sqrt{2P\rho}$$

where ρ for H_2O is 1 g/cm^3. The Reynolds number is:

$$N_{Re} = \frac{\rho v d}{\mu} = 100 \, d \, \sqrt{2P}$$

where μ_{H_2O} is 10^{-2} poise.

Testing was conducted over a pressure range of approximately 30 to 96 psia, and flow rates of H_2O of approximately 20 to 500 g/sec for the orifices employed in the study plus the 1/8" orifice in the atomizer fabricated for the PETC FEF. Results are plotted in Figure 2 as the C_D values versus Reynolds number. As seen in the figure, the C_D values are fairly constant over a range of N_{Re}, with the exception of the data for the 0.25" orifice. For this orifice, the N_{Re} range of interest is approximately 2.3 - 3.0 x 10^5, to which the data are easily extrapolated. The selected C_D values for use in the present study are:

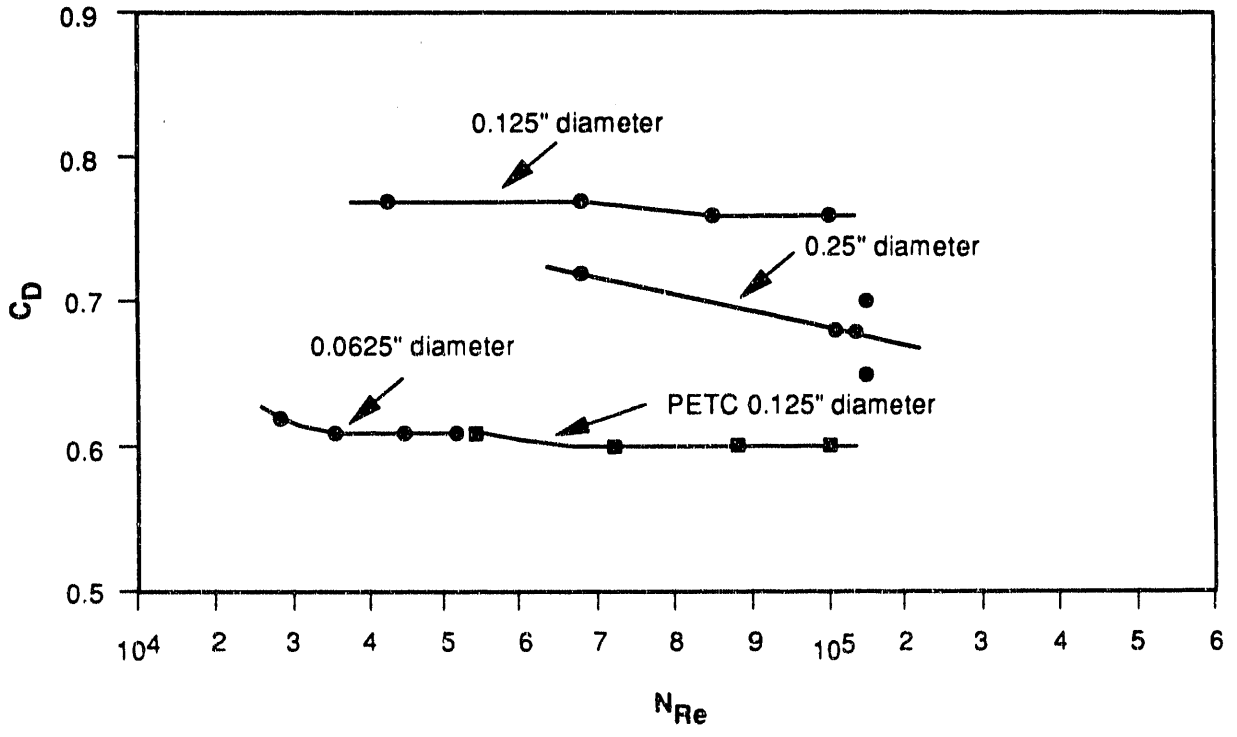

Figure 2

Calibration of Atomizer Air Orifices Using Water

Orifice Diameter (inch)	C_D	β
1/16	0.61	0.17
1/8	0.76	0.33
1/4	0.66	0.66
PETC 1/8	0.60	0.40

These values, although varying among themselves, are in a reasonable range for discharge coefficients as reported in the literature and handbooks. One explanation for the variation is that the upstream configuration of the fittings and hardware of the system has an important effect on the discharge. This may be the case here. For this reason, values of a β parameter are listed in the table. This parameter represents the ratio of the orifice diameter to the pipe diameter in each system.

2.3 Coal and CWF Properties and Production of CWF's for PETC

The coals used in the study were supplied by Energy International, Inc., of Pittsburgh, Pennsylvania. Fuel A was a CWF made from Upper Elkhorn No. 3, an eastern high volatile bituminous A coal. The production lot of CWF was made at 61% solids and diluted as required. The testing in the program was done with a 57% CWF of Fuel A unless otherwise noted.

Fuel B was a CWF of Kemmerer coal, a western subbituminous. The production lot was made at 49% solids and diluted to 45% for testing.

The proximate and ultimate analyses of the coals are listed below, and the particle size distributions of the CWF are also presented. Viscosities of the CWF's are presented in a later section.

Upper Elkhorn No. 3 Coal

Proximate Analysis	Dry Basis
% Ash	2.86
% Volatile	37.60
% Fixed Carbon	59.54
Btu/lb	15,055

Ultimate Analysis	Dry Basis
% Carbon	85.68
% Hydrogen	5.42
% Nitrogen	1.48
% Sulfur	0.60
% Ash	2.86
% Oxygen (diff)	3.96
	100.00

Upper Elkhorn No. 3 CWF (Fuel A)
Particle Size Distribution

Microns	Cumulative % Finer Than	Weight % in Band
21.1	100.0	8.4
14.9	91.7	12.1
10.6	79.6	14.1
7.5	65.5	15.4
5.3	50.2	10.8
3.7	39.4	10.6
2.	28.9	8.2
1.7	20.8	8.6
1.02	12.2	5.7
0.66	6.6	4.9
0.46	1.7	1.2
0.34	0.5	0.0
0.25	0.5	0.0
0.17	0.0	0.0

D_{50} = 5.3 microns

Kemmerer Coal

Proximate Analysis	As Received	Dry Basis
% Moisture	23.06	XXXXX
% Ash	4.13	5.37
% Volatile	35.25	45.81
% Fixed Carbon	37.56	48.82
Btu/lb	9724	12639
% Sulfur	0.53	0.69

Ultimate Analysis	As Received	Dry Basis
% Moisture	23.06	XXXXX
% Carbon	55.80	72.53
% Hydrogen	3.93	5.11
% Nitrogen	1.06	1.38
% Sulfur	0.53	0.69
% Ash	4.13	5.37
% Oxygen (diff)	11.49	14.92
	100.00	100.00

Kemmerer CWF (Fuel B)
Particle Size Distribution

Microns	Cumulati Finer T:	%	Weight % in Band
21.1	100.0		10.2
14.9	89.9		14.1
10.6	75.9		12.5
7.5	63.5		13.6
5.3	50.0		12.1
3.7	38.0		9.6
2.6	28.4		8.5
1.7	19.9		8.3
1.02	11.7		5.9
0.66	5.8		4.1
0.46	1.8		0.9
0.34	0.9		0.0
0.25	0.9		0.0
0.17	0.0		0.0

D_{50} = 5.3 microns

2.4 CWF Nozzle Erosion

During Phase I of this effort (Contract No. DE-AC22-87PC79656), it was noted that the CWF nozzles used in the test rig and the combustion-ready atomizer tended to erode. One of the causes of this erosion was that the material (brass) making up the body of the CWF nozzle was soft and easily eroded. Another problem was that shear rates in the nozzle tended to be high due to the requirement for a high pressure energy (Section 4.0) for good atomization.

In an effort to determine the rate of CWF orifice erosions, and so that a good material could be selected for nozzle construction, an experiment was performed where CWF orifice plates of several sizes and materials were tested for durability. Two materials, hardened carbon steel and silicon nitride, were selected as candidates and three nozzles sizes, 0.025, 0.047, and 0.062 inches diameter (all diameters were ± 0.001 inches). Due to difficulty in manufacturing, only nozzles of 0.025 inches diameter were tested in the silicon nitride material. The nozzles were all placed into holders and were hooked up to a positive displacement pump which recirculated a large quantity of the Fuel "A" (Upper Elkhorn #3 at 57% solids) through them for 100 hours running time. After the test, the nozzles were examined for wear. In none of the cases were the actual hole diameters increased; however, for the hardened steel nozzles, evidence of wear was noted where the edges of the orifice had lost their sharpness. No evidence of wear was noted for the silicon nitride material (Figure 3).

1

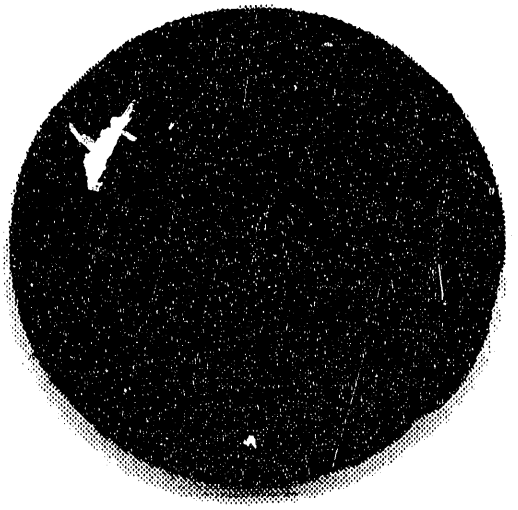

Silicone Nitride
Orifice 0.024"

2

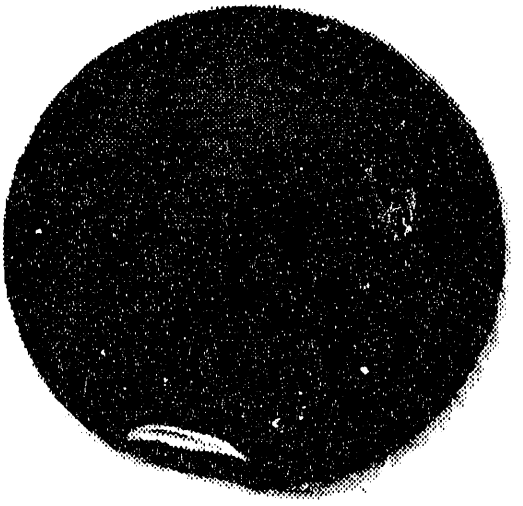

Silicone Nitride
Orifice 0.025"

3

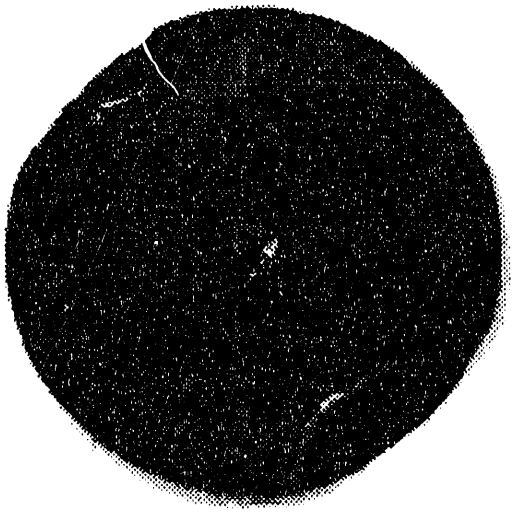

Silicone Nitride
Orifice 0.026"

4

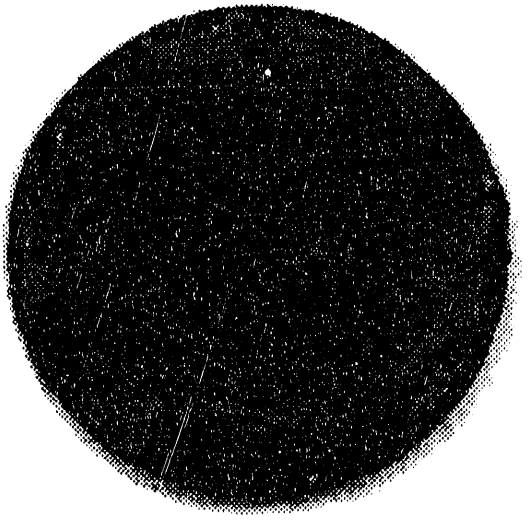

Steel
Orifice 0.026"

Figure 3
Results of Nozzle Erosion Tests

5

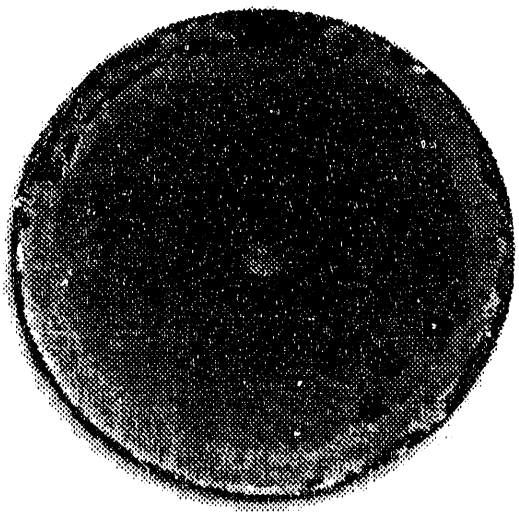

Steel
Orifice 0.062"

6

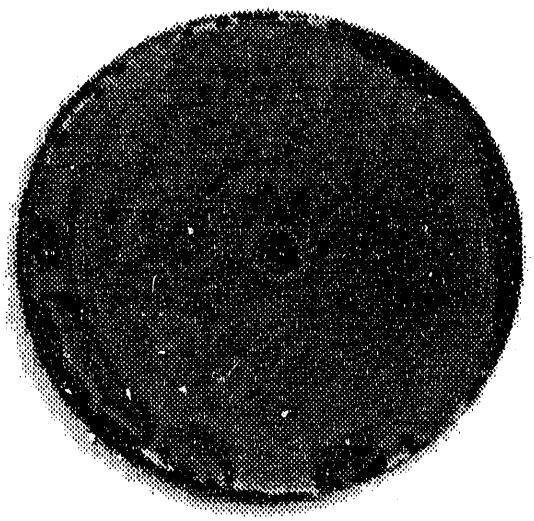

Steel
Orifice 0.047"

8

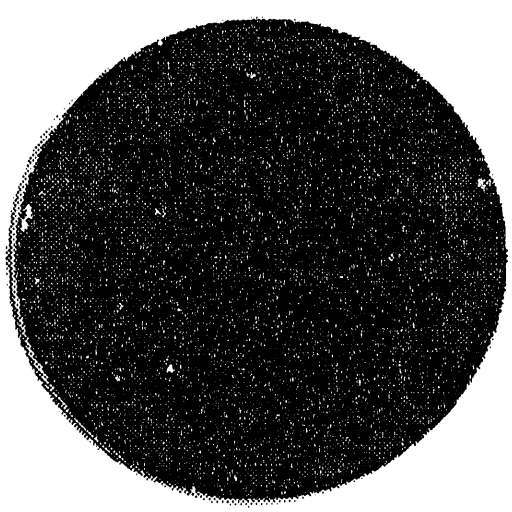

Silicone Nitride
Orifice New 0.025"

Figure 3 (Cont'd)
Results of Nozzle Erosion Tests

3.0 ATOMIZER PERFORMANCE TEST RESULTS

In this section, the results of individual tasks relating to the opposed-jet atomizer and to the Parker Hannifin atomizer are presented.

3.1 Spray Droplet Size Versus Viscosity

Atomization testing for this task was conducted at approximately the 1 MMBTU/H level using a series of Fuel A CWF's in which viscosity was varied by varying the solids content from 61 to 53%. The particle size distribution of the CWF's, as determined by a Microtrac particle size analyzer, is given in the previous section.

Starting with a 61.0% CWF, four other samples were prepared by exact dilution to 59, 57, 55, and 53%. Viscosities were measured with a Burrell-Severs Model A-120 rheometer. This extrusion tube viscometer was used with 0.319- and 0.156-cm orifices. Spray droplet size measurements were also made on these CWF's (except the 61% slurry, which had been found to perform poorly in the atomizer test system) to determine the relationship with viscosity. The rheology of these fuels follows a power law model for non-Newtonian fluid behavior. The relationship between shear stress, τ, and shear rate, $\dot{\gamma}$, is given by the general formula:

$$\tau = K\dot{\gamma}^n$$

which may be rewritten as:

$$\log \tau = \log K + n \log \dot{\gamma}$$

From a plot of $\log \tau$ versus $\log \dot{\gamma}$, the factor $\underline{n}$ is determined, and the constant K is then calculated.

The apparent viscosity, μ, of these fuels is given by the equation $\mu = \tau/\dot{\gamma}$, so that:

$$\text{Apparent viscosity, } \mu = K\dot{\gamma}^{n-1}$$

With an extrusion tube rheometer, shear rate $\dot{\gamma}$ is given by $32\dot{m}/\rho\pi D^3$ where $\dot{m}$ is mass flow of CWF, ρ is density, and D is the diameter of the orifice. Shear stress, τ, is given by $D\Delta P/4L$, where ΔP is the extrusion pressure and L is the length of the orifice. A series of flows are measured at various extrusion pressures, and the resulting data are reduced. A summary of the results is presented in Table 3 in terms of the factors in the above equations.

Table 3. Burrell Viscosity Data

Solids Content	Low Mixing		High Mixing	
	K	n	K	n
61	0.770	1.281	0.257	1.363
59	0.746	1.186	0.622	1.168
57	0.177	1.276	0.310	1.162
55	0.153	1.241	0.394	1.067
53	0.0201	1.437	0.174	1.227

Viscosities calculated from these data will be in units of poise and should be multiplied by 100 to express in centipoise. The two sets presented refer to the same slurries that were subjected to two different levels of mixing. The "low mixing" slurries were thoroughly mixed but at a low shear rate for a short time. The "high mixing" slurries were mixed for two minutes with a high speed turbine mixer. Actual shear rates could not be determined for the mixing processes. As has been reported often in the literature, prolonged high shear mixing changes (usually lowers unless carried too far) viscosity of a CWF, and this is found to be the case here. The "high mixing" data of the table show substantially lower viscosities than the "low mixing" data, with the exception of the 53% CWF where the trend is reversed. (Since the exponent values changed with mixing for each CWF, the lower-viscosity trend will not hold over all $\dot{\gamma}$ rates, but is true for the 61-55% CWF's over the range $10^2 - 10^5$ sec^{-1}, except for the 55% CWF below 250 sec^{-1}.)

The viscosity measurements were made over the approximate $\dot{\gamma}$ shear rate ranges for the highly-mixed slurries as tabulated below:

CWF	Viscosity Measurements Over $\dot{\gamma}$ Shear Rate Ranges (sec^{-1})
61	600 - 6,500
59	3400 - 8,400
57	900 - 26,000
55	1,300 - 13,000
53	400 - 6,100

The highly-mixed CWF's are of interest here because these types were used in the testing. The apparent viscosity versus shear rate $\dot{\gamma}$ is plotted in Figure 4 on log-log scale over the range 10^2 - 10^4 sec^{-1} for the highly-mixed slurries. The trend of decreasing viscosity as well as decreasing exponent n is violated by the 53% CWF, for unknown reasons. All the CWF's are slightly dilatant.

The atomization data for the foregoing CWF's are collected in Table 4 where duplicate sets are listed corresponding to two different positions of the laser beam in the sprays.

Table 4. Atomization Spray Data for CWF's of Measured Viscosity

			Position I			Position II		
Solids	Psia	A/F	D_{80}	D_{50}	D_{20}	D_{80}	D_{50}	D_{20}
53%	55	.31	46	32	20	47	32	20
	75	.42	40	26	14	42	27	16
	95	.53	38	24	14	39	25	15
	115	.65	37	24	12	36	24	12
55%	55	.31	50	34	21	49	33	21
	75	.42	45	29	18	42	28	17
	95	.53	44	27	16	43	26	16
	115	.64	42	25	16	41	25	15
57%	55	.31	48	32	21	49	33	21
	75	.42	45	29	17	45	30	19
	95	.54	39	26	14	43	28	17
	115	.65	41	27	15	42	27	16
59%	55	.29	63	37	22	58	36	22
	75	.39	50	30	19	53	33	20
	95	.50	53	32	19	53	33	20
	115	.60	44	27	16	48	30	19

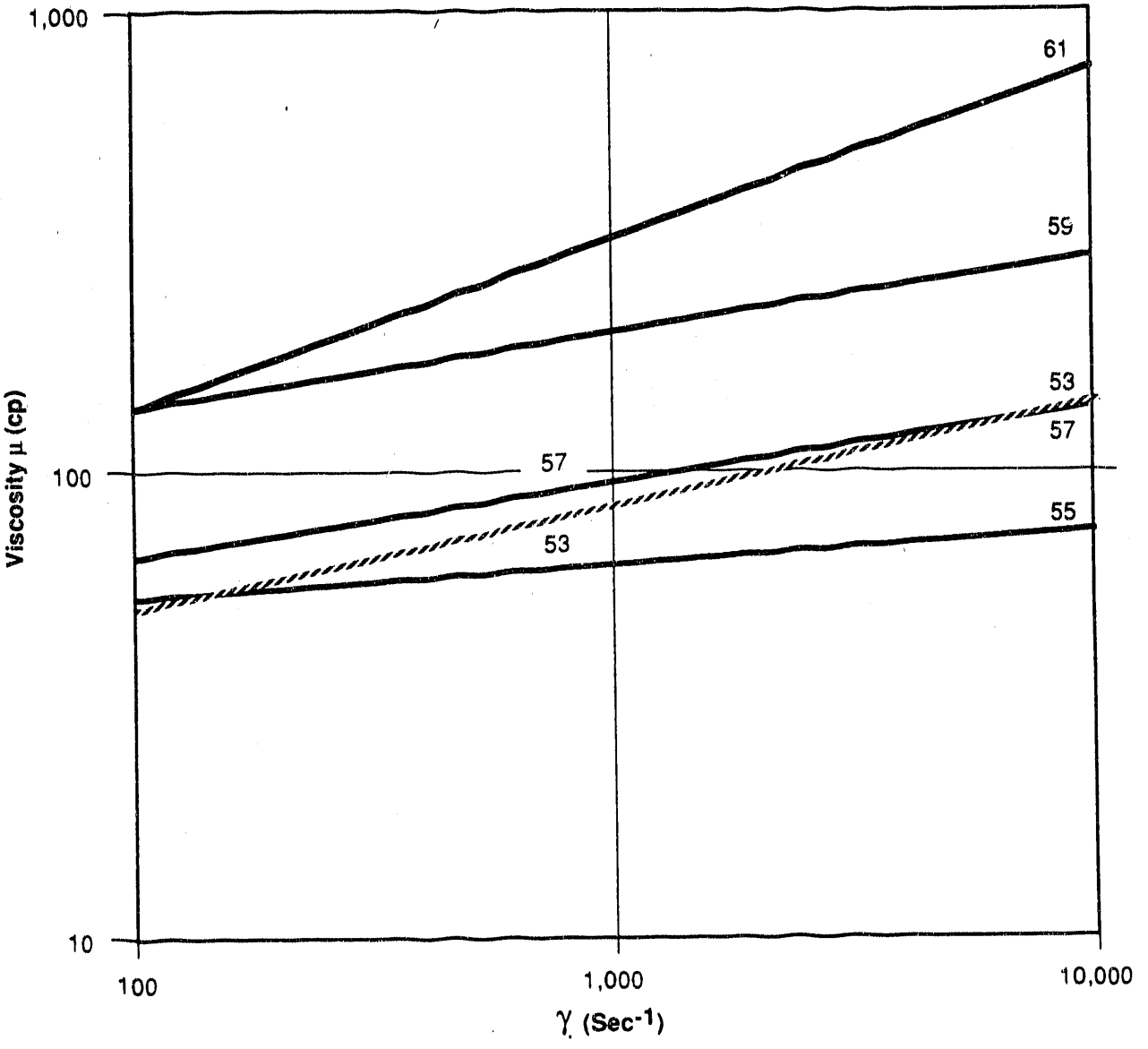

Figure 4

Viscosity Versus Shear Rate for Well-Mixed CWF's at Varying Solids Contents

In Figure 5, the averaged MMD values are plotted versus the slurry viscosities at low (100 sec^{-1}) and high (10^4 sec^{-1}) shear rates. There is an overall trend, independent of shear rate, of increasing droplet size with increasing viscosity; however, a trend is not discernible at low viscosities alone. The results at low viscosities were borne out by the handling operations in the laboratory and the actual atomization testing, where it was apparent that the 53, 55, and 57% slurries all seemed to behave about the same.

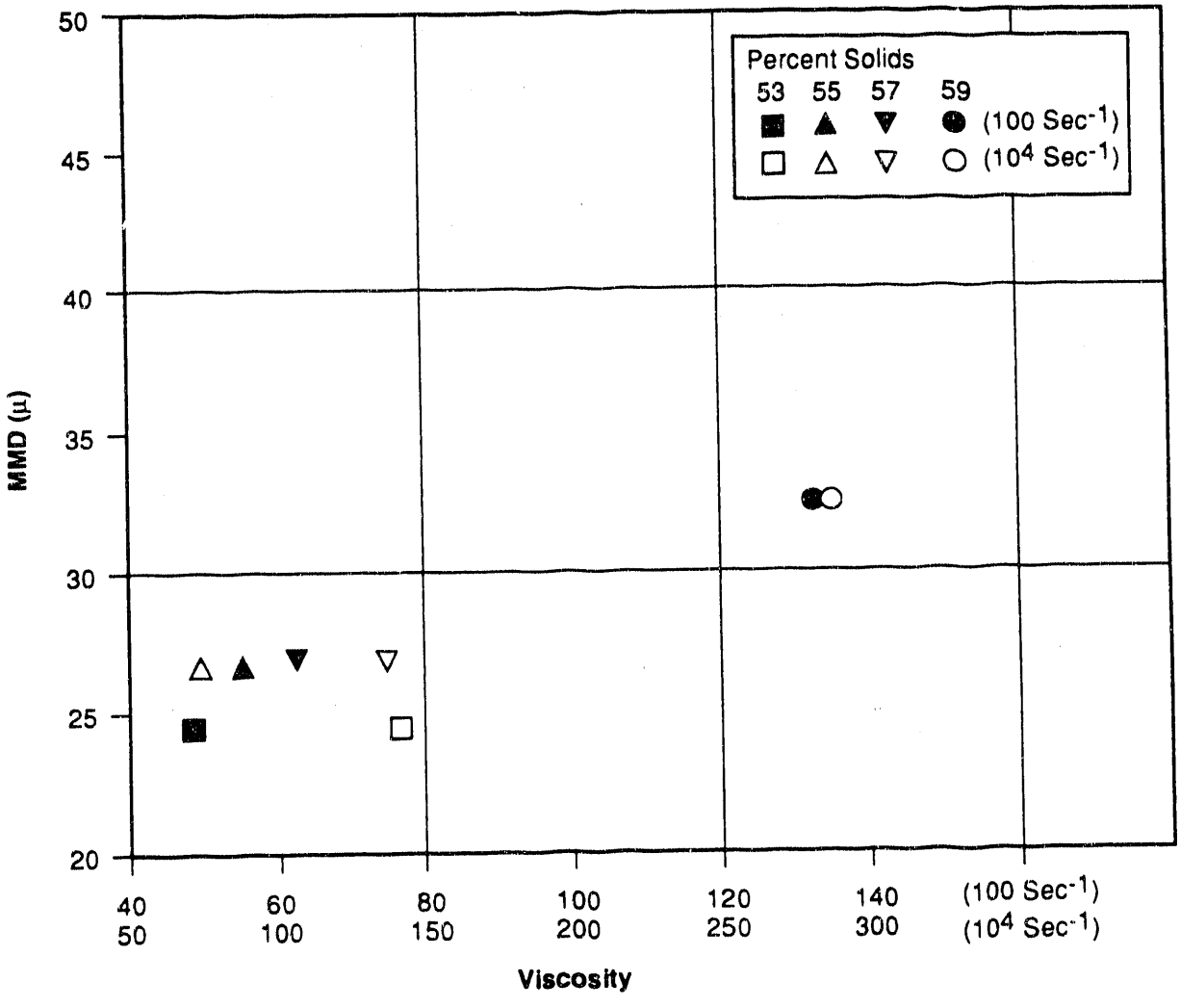

Figure 5

Plot of Averaged MMD Values Versus Viscosity at Low Shear Rate (100 Sec^{-1}) and at High Shear Rate (10^4 Sec^{-1})

3.2 Parker Hannifin Atomizer Testing

An evaluation of a commercial atomizer was undertaken for comparison with the opposed-jet unit. The atomizer chosen was a Parker Hannifin "Viscosity Insensitive Prefilmer (VIP)" external type. A schematic diagram is shown in Figure 6. The device operates by sandwiching CWF flow between two air flows. One air flow is through the central orifice, CWF flow is through a surrounding annular opening, and the second air flow is through an outer annular opening. All three flows are swirled, the inner air parallel with CWF swirl, and the outer air swirl opposite to that of the CWF. Performance of the atomizer has been reported by R. V. Jones ("The Design and Testing of a Dual Fuel Coal Water Slurry Atomizer for a Coal-Fired Gas Turbine," Fourteenth International Conference on Coal and Slurry Technology, p. 167, 1989) and by B. G. Miller, et al. ("An Update of Penn State's Superclean Coal-Water Slurry Demonstration Program," Sixteenth International Conference on Coal and Slurry Technologies, p. 587, 1991).

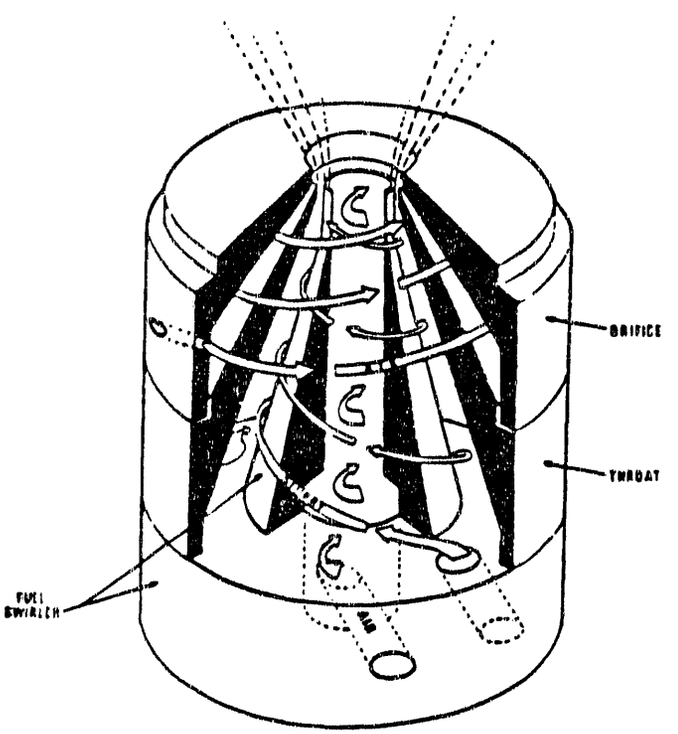

Figure 6
Schematic of Parker Hannifin VIP Atomizer

Results of the evaluation are summarized in Table 5 and in Figure 7. The data presented represent the best performance obtained with the Parker Hannifin unit and refer to a capacity of 11 g/sec of an approximately 57% CWF, with less than 100 cp viscosity at 100 sec^{-1} shear rate. (11 g/sec of this CWF is equivalent to 0.75 MMBTU/H; according to the vendor, the unit was sized for 0.5 MMBTU/H with turnup and turndown capacity.) Tests were performed at $\dot{m}_{CWF}$ of 2.8 to 30.7 g/sec, and A/F ratios of 0.1 to 4.5. (These A/F ratios were calculated assuming a C_D = 1.0.)

Table 5. Summary of Results of Testing Parker Hannifin Atomizer with CWF

Psia	135	115	95	135	75	115
A/F	1.14	0.97	0.81	0.67	0.63	0.57
D_{80}	30	37	107	172	>564	>564
D_{50}	22	27	34	81	99	112
D_{20}	13	16	20	33	29	39

In summary, we found that very fine droplet sprays, down to 22 microns MMD, can be achieved; however, an A/F ratio of over 1.1 was required. An even more serious problem, however, was plugging of the atomizer after a short period of operation during every test series. By the end of each test series, the atomizer outlet was partially blocked with dried CWF in several of the air passages and was producing an erratic spray. Attempts to identify the cause of this problem and correct it were unsuccessful. Our best assessment of the problem is that the high degree of swirl of the atomizing air creates a strong vortex with a low-pressure area near the atomizer face and an accompanying recirculation flow. The overall effect is to draw CWF back into the air channels, which, while only a relatively small amount of CWF is involved, is nevertheless enough to cause partial blockage after a period of time. Reports in the literature (two references cited above) seem to hint at this problem with the Parker Hannifin atomizer.

3.3 PETC Opposed-Jet Atomizer Unit

An operational opposed-jet atomizer was fabricated for use by PETC in the Fuel Evaluation Facility. This was patterned after the atomizer that

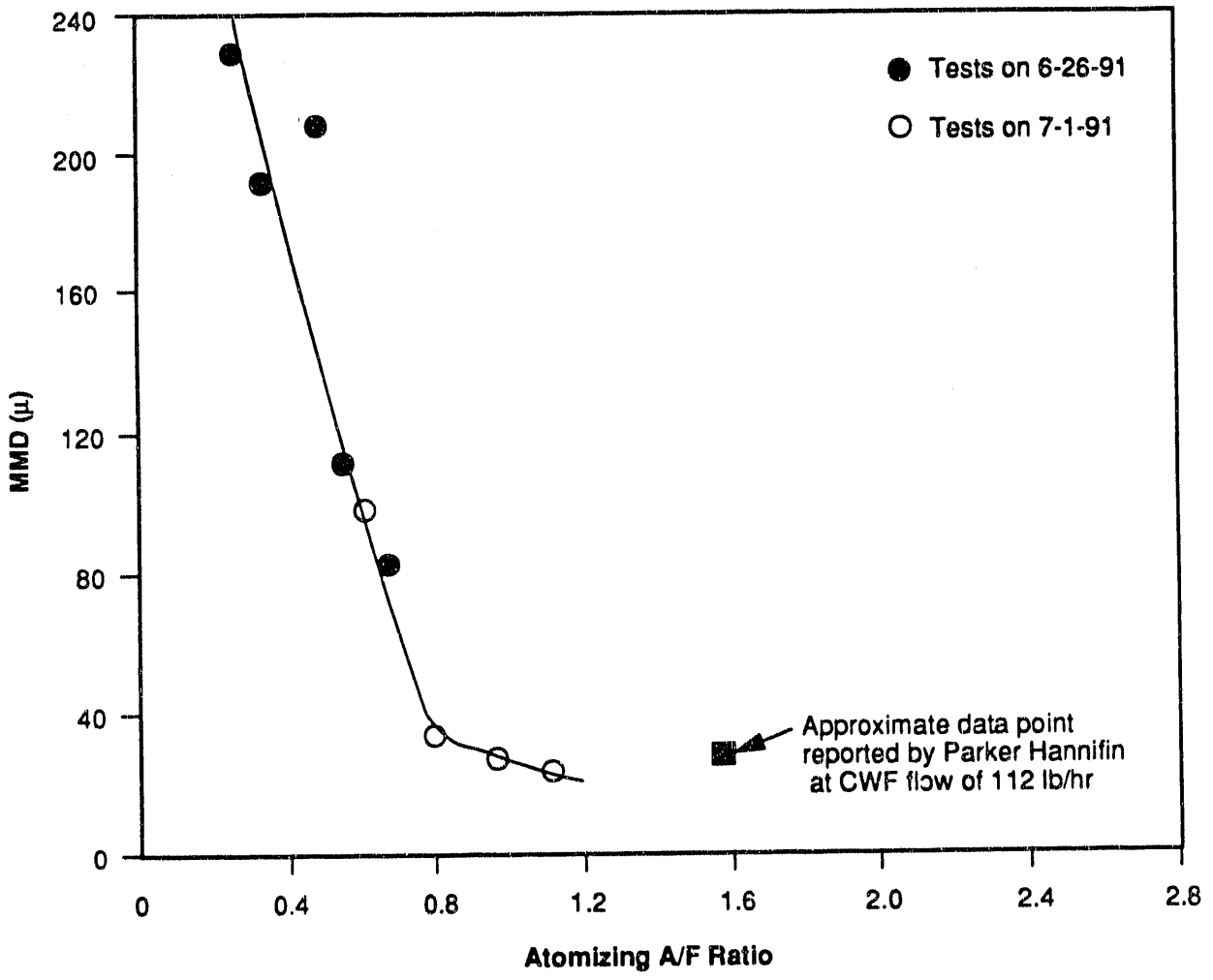

Figure 7

Parker Hannifin Atomizer at CWF Flow of 88 lb/hr (Equivalent to 0.75MMBtu/H) of a 57% CWF. Viscosity <100 CP at 100 Sec^{-1}

was used by Atlantic Research in the previous, Phase I program. Modifications versus the ARC unit included reducing the outside diameter from 4" to 1-7/8" in order to fit the FEF diffuser. This necessitated eliminating some of the water cooling, and also reducing the distance between the CWF orifices to about 1-1/2" from 2". This PETC unit is to be operated at 0.5 MMBTU/H; however, it was not possible to reduce the CWF orifice diameters to an optimum size of about 0.015" or less because testing had shown that blockage by CWF occurred at this small size. The CWF orifices are removable, and two sizes were tested (0.020" and 0.025") with no meaningful difference being found in spray droplet size. The atomizing air orifice size was 0.125", and two inserts were machined and tested - one that provided a distance of 4 mm between the air orifice and the CWF collision zone; and one that provided a distance of 9 mm. Testing showed that there was no significant difference between the two.

It can be reported that there were no CWF flow problems encountered with the PETC unit when operated with Fuel A at 55 and 57% solids content. With Fuel B at 49% solids, blockage of the 70 mesh basket screens, that are used in-line with the atomizer, did occur. When the solids content was reduced to 45%, there were no blockage problems that completely stopped the flow during testing. However, it was observed that each time a test series was run with the 45% CWF, the flow rate dropped continuously from start to finish. For example, over approximately a 15-minute period in one test series, the flow progressively decreased from 10.1 g/sec to 7.5 g/sec. Fuel B behaved like a typical CWF made from a low-rank coal in that it exhibited a strong tendency to gel under conditions of little or no shear. The basket screens after some usage with any fuel tend to develop a thick dilatant deposit inside. With Fuel B, this deposit appeared to be a thin but very cohesive coating on the inside of the baskets. This coating was attributed to the gelling tendency (Bingham plasticity) of Fuel B, and it was judged to be more impervious to CWF flow than the deposit from Fuel A.

In the Phase I program, it was found that during combustion testing, a deposit of dried slurry built up on the face of the atomizer. In order to avoid this, an attachment consisting of a flat plate was placed on the front of the atomizer. In the present program, one of the objectives of the testing

was to observe this buildup under cold-flow conditions and to evaluate attachments of different designs for eliminating it. In addition to a flat plate, a nozzle was also fabricated. This nozzle had a 1" opening to allow atomized CWF to discharge as an unimpeded spray. It was approximately 1" in length with beveled sides to direct the flow of exterior air parallel to the spray direction. A moderate buildup of CWF on the front of the atomizer was still observed.

Results of tests with the PETC unit are collected in the eight test groupings that comprise Table 6. Only MMD values are reported here for ease of interpretation; the D_{80}, D_{50}, and D_{20} values are listed in Appendix C. Test Groups 1, 2, and 3 represent results of the atomizer operating with Fuel A at approximately 1 MMBTU/H. The attachment on the face of the atomizer was changed from (1) no attachment, to (2) a nozzle extension with a 1" diameter opening, to (3) a flat plate with a 5/8" diameter opening. The finest sprays were observed with the 5/8" plate; however, as noted later, this plate tended to produce some very coarse droplets.

In Test Series 4 and 5, the atomizer capacity was reduced to 0.66 MMBTU/H with Fuel A, and droplet sizes were measured with the nozzle attachment and the flat plate. Again, the flat plate with a 5/8" diameter opening was found to produce sprays of finer droplets. However, quite a large fraction of the CWF (between 5 and 18%) was poorly atomized as droplets of large diameter (260-560 microns). These would burn very poorly in a combustor and lead to low carbon burnout. The nozzle extension is, therefore, to be favored over the flat plate, assuming no other unforeseen problems arise in actual combustion testing.

In Test Series 6 and 7, Fuel A was again employed (at a slightly higher capacity - 0.73 versus 0.66 MMBTU/H), the CWF orifice diameter was changed (0.020" from 0.025"), and the distance of the air orifice to the collision zone was changed (from 4 mm to 9 mm). Test Series 6 can be compared directly to Series 4, and the conclusion drawn that there was no meaningful change in the spray droplet size between 0.020" and 0.025" CWF orifices. Test Series 7 versus Series 6 showed that increasing the air-orifice-to-collision-

Table 6. Summary of Data From PETC Opposed-Jet Atomizer Unit

1. Fuel A 55% CWF
   Rate = 14.3 g/s
   = 0.95 MMBTU/H

   CWF orifices 0.025", air orifice 0.125", Distance air orifice to collision zone 4 mm, No attachment on face of atomizer

Pressure (psia)	A/F	MMD (microns)
55	.29	47, 46
75	.39	40, 40
95	.49	39, 38
115	.60	37, 36

2. Fuel A 55% CWF
   Rate = 14.3 g/s
   = 0.95 MMBTU/H

   CWF orifices 0.025", air orifice 0.125", Distance air orifice to collision zone 4 mm, Nozzle extension with 1" diameter opening on face of atomizer

Pressure (psia)	A/F	MMD (microns)
55	.29	61
75	.39	42
95	.49	37
115	.60	30, 21*

3. Fuel A 55% CWF
   Rate = 14.3 g/s
   = 0.95 MMBTU/H

   CWF orifices 0.025", air orifice 0.125", Distance air orifice to collision zone 4 mm, Flat plate with a 5/8" diameter opening on face of atomizer**

Pressure (psia)	A/F	MMD (microns)
55	.29	38
75	.39	26
95	.49	22
115	.60	20

---

*This test was run in duplicate, but in the second experiment the laser was directed through a different position in the spray.

**Laser position in spray corresponds to that of first four tests of previous series, not the test with the asterisk. Slight amount of material showed in highest band of Malvern analyzer (260-560 microns).

Table 6. Summary of Data From PETC Opposed-Jet Atomizer Unit (Cont'd)

4. Fuel A 55% CWF
   Rate = 10.0 g/s
   = 0.66 MMBTU/H

CWF orifices 0.025", air orifice 0.125", Distance air orifice to collision zone 4 mm, 1" diameter nozzle extension on atomizer

Pressure (psia)	A/F	MMD (microns)
55	.41	50
75	.56	42
95	.70	41
115	.85	38

5. Fuel A 55% CWF
   Rate = 10.0 g/s
   = 0.66 MMBTU/H

CWF orifices 0.025", air orifice 0.125", Distance air orifice to collision zone 4 mm, Flat plate with 5/8" opening on face of atomizer***

Pressure (psia)	A/F	MMD (microns)
55	.41	32
75	.56	26
95	.70	23
115	.85	28

6. Fuel A 57% CWF
   Rate = 10.7 g/s
   = 0.73 MMBTU/H

CWF orifices 0.020", air orifice 0.125", Distance air orifice to collision zone 4 mm, 1" diameter nozzle extension on atomizer

Pressure (psia)	A/F	MMD (microns)
55	.38	48
75	.52	41
95	.65	41
115	.79	40

***In these tests with flat plates, there was between 5 and 18% of the spray droplets in the largest band (260-560 microns) of the Malvern analyzer, indicating that large droplets were passing through the laser. These were only found when the flat plate was used.

Table 6. Summary of Data From PETC Opposed-Jet Atomizer Unit (Cont'd)

7. Fuel A 57% CWF
   Rate = 0.7 g/s
   = 0.73 MMBTU/H

CWF orifices 0.020", air orifice 0.125",
Distance air orifice to collision zone 9 mm,
1" diameter nozzle extension on atomizer

Pressure (psia)	A/F	MMD (microns)
55	.38	54, 50
75	.52	47, 46
95	.65	40, 39
115	.79	35, 37

8. Fuel B 45% CWF
   Rate = 8.4 g/s
   = 0.38 MMBTU/H

CWF orifices 0.020", air orifice 0.125",
Distance air orifice to collision zone 9 mm,
1" diameter nozzle extension on atomizer

Pressure (psia)	A/F	MMD (microns)
55	.49	26, 25
75	.66	22, 21
95	.84	21, 22
115	1.02	20, 20

zone distance to 9 mm from 4 mm also produced no significant changes in droplet size.

The last set of data in Table 6, Test Series 8, was obtained with Fuel B at 45% solids. The droplet sizes in the table are remarkably fine, and presumably this is attributable to the high level of dilution of this CWF required to prevent blockage of the filtering screens.

3.4 Slotted Air Orifices

Employing slotted atomizing air orifices, the atomizer was evaluated at approximately 1 MMBTU/H capacity using an approximately 57% CWF of 250 cp viscosity at 100 sec^{-1}, made from Upper Elkborn No. 3 coal. The comparison was made against the atomizer operating with a circular air orifice of approximately the same cross-sectional area. The slotted orifice was oriented both vertically and horizontally. With the slot oriented vertically, performance was poorer than with the circular orifice at low atomizing A/F ratios, and about equal at high A/F ratios, the dividing line being an A/F of approximately 0.7. With the slot oriented horizontally, the performance was slightly better than with the circular orifice at low A/F ratios and about equal at high A/F ratios.

The foregoing qualitative summary of the performance of the slotted atomizing air orifice is based on the experimental data summarized in Table 7. It is noted that the cross-sectional areas of the slotted and circular orifices were not exactly the same. The circular orifice had an area of 0.079 cm^2, and the slotted orifice 0.090 cm^2, or 14% greater. (The aspect ratio of L/D for the slotted orifice was 4.0.) Thus, when comparing the tabulated data, some allowance should be made for this area difference. The atomizing air mass flow rates, $\dot{m}_a$, were estimated from the relationship, described earlier, for choked flow through a critical orifice. This procedure seemed adequate to estimate the atomizing A/F ratios reported here. The summary in Table 7 represents averages of D_{50} values of sprays taken from the more complete data presented in Table 8. These data include the D_{80}, D_{50}, and D_{20}, measured values for 12 separate sets of tests at four pressures.

Table 7. Summary of Averaged Spray Droplet Measurements for Slotted and Circular Atomizing Air Orifices at CWF Capacity of 1 MMBTU/H ($\dot{m}_{CWF}$ = 16.7 g/s)

	A/F		D_{50} (microns)		
Psia	Slotted	Circular	□	○	▭
55	0.47	0.41	91	38	34
75	0.64	0.56	38	32	29
95	0.80	0.70	29	29	28
115	0.97	0.85	26	28	29

Table 8. Spray Droplet Measurements for Slotted and Circular Atomizing Air Orifices at CWF Capacity of 1 MMBTU/H ($\dot{m}_{CWF}$ = 16.7 g/s)

Psia	A/F* Slotted	A/F* Circular	D_{80} / D_{50} / D_{20} (microns)											
			□					○				▭		
55	0.47	0.41	217	>564	222	>564	>564	70	58	61	55	61	63	61
			58	108	63	109	116	40	36	38	37	34	34	33
			23	30	27	29	30	24	21	21	21	17	17	17
75	0.64	0.56	61	100	80	58	72	48	50	48	54	53	56	50
			33	44	42	34	37	32	31	31	34	29	29	28
			18	22	21	19	20	19	18	18	18	14	14	13
95	0.80	0.70	46	48	47	44	46	45	46	45	49	58	57	55
			28	28	29	28	31	30	28	28	29	29	28	28
			17	15	16	16	17	16	15	15	15	13	12	13
115	0.97	0.85	41	42	41	43	45	43	47	44	52	62	58	58
			25	26	25	26	28	29	28	26	30	30	28	30
			16	14	13	14	15	15	15	14	15	13	13	14

*Data not corrected for a discharge coefficient (C_D) because only a value for circular orifice is known.

Based on these experiments with CWF, there appears to be little or no improvement to be achieved by changing the configuration of the atomizing air orifice. However, this conclusion remains somewhat uncertain for the following reason. Prior to conducting the tests with the slotted orifices and CWF, testing was performed using water as the fluid to be atomized, and comparisons were made between results with the circular and slotted air orifices. With the slotted air orifice oriented horizontally, an improvement in water atomization was observed relative to the circular orifice. For this case, the D_{50} values decreased from about 10 to 8 microns at A/F ratios in the range of 0.6. With the slotted orifice oriented vertically, a substantially greater improvement was observed with water, down to less than 6 microns. The lower limit of the droplet size analyzer was approximately 6 microns, hence it was not possible to determine exactly what these D_{50} values were. However, the trend of these results with water was not observed with the CWF as reported above In view of this unexplained discrepancy, further experiments may be warranted.

3.5 Opposed-Jet Small-Scale Testing

The opposed-jet atomizer was evaluated for use at lower capacity than 1 MMBTU/H using a circular atomizing air orifice. The objective was to attempt to reach a lower scale of operation of 0.1 MMBTU/H; but as mentioned below, testing was only successful down to 0.24 MMBTU/H. An air orifice of 1/16" diameter, 0.020 cm^2 area, one-quarter the area employed at 1 MMBTU/H, was used. Initial testing was done with CWF orifices of 0.012" diameter, but these became plugged very soon after each test was started, even with CWF diluted to 53% solids. Accordingly, testing had to be conducted with larger orifices, and the next available size was 0.018" diameter. This size performed satisfactorily with no plugging problems, even with 57% CWF which was used in the testing.

Results are summarized in Table 9 where conditions and spray droplet MMDs are presented. At a CWF flow rate of 3.5 g/sec, equivalent to 0.24 MMBTU/H, the best mass median diameters attained for the sprays were 60 microns at an A/F ratio of 0.24. At higher and lower A/F, the MMDs were larger. At a CWF flow rate of 5.8 g/sec, equivalent to 0.40 MMBTU/H, the MMDs

Table 9. Summary of Results of Opposed-Jet Atomizer at Low Capacity

Capacity: 0.24 MMBTU/H (3.5 g/sec)

Psia	25	35	45	55	65*	75
A/F	0.22	0.31	0.40	0.49	0.57	0.66
D_{80}	157	119	106	128	110	122
D_{50}	126	70	60	70	64	73
D_{20}	61	38	29	32	28	36

Capacity: 0.40 MMBTU/H (5.8 g/sec)

Psia	55	75	95	11[illegible]*
A/F	0.29	0.40	0.51	0.[illegible]
D_{80}	80	77	78	87
D_{50}	46	45	44	46
D_{20}	24	21	20	20

*At these air pressures, the CWF jets were not able to penetrate the atomizing air blast. Data at 0.4 MMBTU/H are average of three runs.

minimized at 44 microns at an A/F of approximately 0.31. Actually, there was no statistically meaningful difference for MMDs over the full range of A/F ratios tested at 0.4 MMBTU/H. In Table 9, it is noted that at sufficiently high pressure, the CWF jets were not able to penetrate the atomizing air blasts, as observed visually. This penetration is a necessary condition for good atomization and is addressed later.

The small-scale results are consistent with droplet MMDs of 20-30 microns that are achieved at 1 MMBTU/H level at A/F ratios of about 0.5-0.6 using this CWF. The conclusion to be drawn from the testing is that the opposed-jet atomizer can probably be operated down to about 200,000 Btu/H with some sacrifice of spray droplet size.

3.6 Opposed-Jet Large-Scale Testing

The opposed jet atomizer was also evaluated at higher capacity than the baseline level of 1 MMBTU/H. Tests were conducted at 2.86 and 4.3 MMBTU/H, which were the highest levels achievable owing to equipment limitations, mainly the capacity of the air compressor. An air orifice of 0.25" diameter (0.317 cm^2 area, or four times the area employed at 1 MMBTU/H) was used. The CWF orifice diameter was 0.039" (0.00771 cm^2) at 2.86 MMBTU/H and 0.0465" (0.0110 cm^2) at 4.3 MMBTU/H. A 57% solids CWF (Fuel A) was used in all tests. Testing was also performed with a Fuel C, which was a coarser grind and more highly-loaded slurry than Fuel A. However, this testing was unsuccessful because of problems with the fuel and with the particle analysis equipment. It was not possible to conduct the testing over again because of time limitations at the end of the program.

Results of the larger-scale testing with Fuel A are summarized in Table 10. As the scale of the testing increased from 2.86 to 4.3 MMBTU/H, the droplet sizes decreased. The MMDs at the higher scale were the smallest achieved. The variation in MMD between sets at 4.3 MMBTU/H is probably real and due to the laser beam traversing different locations in the sprays. The MMDs at 4.3 MMBTU/H are plotted in Figure 8 versus A/F ratio to illustrate the spread of the data. It is apparent from a comparison of small- and large-scale results that the opposed-jet atomizer performs increasingly better as the scale of operation increases.

Table 10. Summary of Results of Opposed-Jet Atomizer at Larger Capacity

Capacity: 2.86 MMBTU/H (41.8 g/sec)

Psia	45	55	65	75	82
A/F	0.35	0.43	0.51	0.58	0.64
D_{80}	76	58	47	47	43
D_{50}	38	32	27	26	24
D_{20}	20	16	13	12	13

Capacity: 4.3 MMBTU/H (63.3 g/sec)

Set 1

Psia	55	75	87	88
A/F	0.29	0.39	0.45	0.45
D_{80}	73	33	31	45
D_{50}	31	18	17	19
D_{20}	14	9	7	9

Set 2

Psia	55	65	75	82	85
A/F	0.29	0.33	0.39	0.42	0.44
D_{80}	65	46	41	38	41
D_{50}	32	25	23	21	22
D_{20}	16	12	11	10	11

Set 3

Psia	55	65	75	95
A/F	0.29	0.33	0.39	0.50
D_{80}	71	49	46	40
D_{50}	34	27	24	23
D_{20}	16	13	11	10

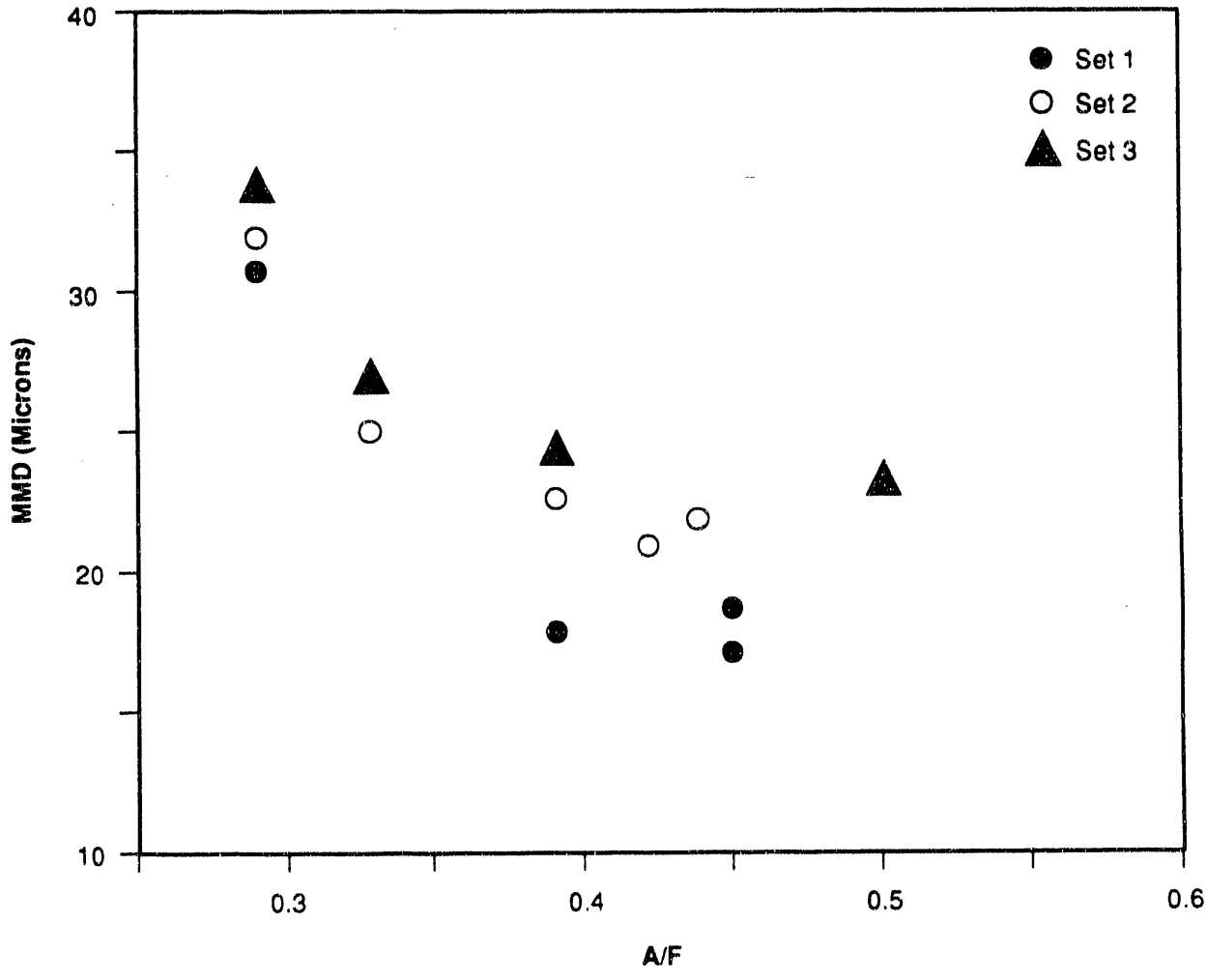

Figure 8

Plot of MMD Data at 4.3MMBtu/H

4.0 ANALYSIS OF OPPOSED-JET ATOMIZATION PROCESS

The atomization data have been modeled in terms of gas dynamic concepts in order to provide an understanding of the opposed-jet process and a basis for design predictions. Based on experience gained in the testing of the atomizer, it was determined that there are three conditions necessary for production of a fine particle spray:

- Sufficient atomization air in relation to the quantity of fuel being fired (i.e., sufficient atomizing A/F ratio).
- Adequate pressure energy (i.e., force per unit area) of the atomization air blast.
- Adequate pressure energy of the CWF jets so they can penetrate the air blast stream.

To briefly expand on these requirements - the conditions specify that not only must the atomization A/F ratio be sufficiently high, but the strength of the air blast must also be adequate to shatter the CWF into fine droplets. The third condition is required because it has been observed that if the CWF jets are not forceful enough, they will not penetrate into the atomization air blast. This results in CWF flowing mostly along the edges of the air stream, with poor atomization being produced by inefficient parallel shear action. In the analysis that follows, some quantitative specifications are put on the foregoing conditions based on gas dynamic relations.

The data on which the analysis is based are summarized in Table 11 in five sets that represent testing from capacity equivalent to 0.24 up to 4.3 MMBTU/H, under cold flow conditions. The parameters of orifice size and CWF and air flow rates were varied over a wide range which provided substantial variation in the required quantities of A/F ratio, density and velocity needed in the analysis. The symbols in the table represent:

Table 11. Summary of Data at Different Atomization Capacities Used for Modeling

Capacity: 0.24 MMBTU/H

Orifices: D_F = 0.018", $A_F = 1.64 \times 10^{-3}$ cm^2

D_A = 1/16", $A_A = 1.98 \times 10^{-3}$ cm^2, C_D = 0.61

$\dot{m}_F$: 3.5 g/sec total, 1.75 g/sec per orifice

$(1/2\ \rho v^2)_F$: 0.49×10^6 dynes/cm^2, T_t = 250°K, v_t = 31,655 cm/sec

A/F	P_u (psia)	P_t (psia)	ρ_t (g/cm^3)	$(1/2\ \rho v^2)_A \times 10^6$ (dy/cm^2)	$(1/2\ \rho v^2)_{F/A}$	MMD (μ)
0.13	25	13.2	0.00127	0.64	0.76	126
0.19	35	18.5	0.00178	0.89	0.55	70
0.24	45	23.8	0.00229	1.15	0.42	60
0.29	55	29.1	0.00280	1.40	0.35	70
0.34	65	34.3	0.00330	1.65	0.29	64
0.40	75	39.6	0.00381	1.91	0.26	73

Capacity: 0.40 MMBTU/H

Orifices: D_F = 0.018", $A_F = 1.64 \times 10^{-3}$ cm^2

D_A = 1/16", $A_A = 1.98 \times 10^{-3}$ cm^2, C_D = 0.61

$\dot{m}_F$: 5.8 g/sec total, 2.9 g/sec per orifice

$(1/2\ \rho v^2)_F$: 1.34×10^6 dynes/cm^2, T_t = 250°K, v_t = 31,655 cm/sec

A/F	P_u (psia)	P_t (psia)	ρ_t (g/cm^3)	$(1/2\ \rho v^2)_A \times 10^6$ (dy/cm^2)	$(1/2\ \rho v^2)_{F/A}$	MMD (μ)
0.18	55	29.0	0.00279	1.40	0.96	46
0.24	75	29.6	0.00381	1.91	0.70	45
0.31	95	50.2	0.00483	2.42	0.55	44
0.37	115	60.7	0.00584	2.93	0.46	46

Table 11. Summary of Data at Different Atomization Capacities Used for Modeling (Cont'd)

Capacity: 1.1 MMBTU/H

Orifices: D_F = 0.024", $A_F = 2.9 \times 10^{-3}$ cm^2

D_A = 1/8", $A_A = 7.9 \times 10^{-2}$ cm^2, C_D = 0.76

$\dot{m}_F$: 16.6 g/sec total, 8.3 g/sec per orifice

$(1/2\ \rho v^2)_F$: 3.50×10^6 dynes/cm^2, T_t = 250°K, v_t = 31,655 cm/sec

A/F	P_u (psia)	P_t (psia)	ρ_t (g/cm^3)	$(1/2\ \rho v^2)_A \times 10^6$ (dy/cm^2)	$(1/2\ \rho v^2)_{F/A}$	MMD (μ)
0.31	55	29.0	0.00279	1.40	2.48	33
0.42	75	39.6	0.00381	1.91	1.85	30
0.54	95	50.2	0.00483	2.42	1.44	27
0.65	115	60.7	0.00584	2.93	1.20	27

Capacity: 2.86 MMBTU/H

Orifices: D_F = 0.039", $A_F = 7.71 \times 10^{-3}$ cm^2

D_A = 1/4", A_A = 0.317 cm^2, C_D = 0.66

$\dot{m}_F$: 41.8 g/sec total, 20.9 g/sec per orifice

$(1/2\ \rho v^2)_F$: 3.14×10^6 dynes/cm^2, T_t = 250°K, v_t = 31,655 cm/sec

A/F	P_u (psia)	P_t (psia)	ρ_t (g/cm^3)	$(1/2\ \rho v^2)_A \times 10^6$ (dy/cm^2)	$(1/2\ \rho v^2)_{F/A}$	MMD (μ)
0.35	45	23.8	0.00229	1.15	2.70	38
0.43	55	29.0	0.00279	1.40	2.22	32
0.51	65	34.3	0.00330	1.65	1.89	27
0.58	75	39.6	0.00381	1.91	1.64	26
0.64	82	43.3	0.00417	2.09	1.49	24

Table 11. Summary of Data at Different Atomization Capacities Used for Modeling (Cont'd)

Capacity: 4.3 MMBTU/H

Orifices: D_F = 0.0465", A_F = 1.10 x 10^{-2} cm^2

D_A = 1/4", A_A = 0.317 cm^2, C_D = 0.66

$\dot{m}_F$: 63.3 g/sec total, 31.7 g/sec per orifice

$(1/2\ \rho v^2)_F$: 3.55 x 10^6 dynes/cm^2, T_t = 250°K, v_t = 31,655 cm/sec

A/F	P_u (psia)	P_t (psia)	ρ_t (g/cm^3)	$(1/2\ \rho v^2)_A \times 10^6$ (dy/cm^2)	$(1/2\ \rho v^2)_{F/A}$	MMD (μ)
0.29	55	29.0	0.00279	1.40	2.54	31
0.39	75	39.6	0.00381	1.91	1.86	18
0.45	87	45.9	0.00442	2.21	1.61	17
0.45	88	46.5	0.00447	2.24	1.58	19
0.29	55	29.0	0.00279	1.40	2.54	32
0.33	65	34.3	0.00330	1.65	2.15	25
0.39	75	39.6	0.00381	1.91	1.86	23
0.42	82	43.3	0.00417	2.09	1.70	21
0.44	85	44.9	0.00432	2.16	1.64	22
0.29	55	29.0	0.00279	1.40	2.54	34
0.33	65	34.3	0.00330	1.65	2.15	27
0.39	75	39.6	0.00381	1.91	1.86	24
0.50	95	50.2	0.00483	2.42	1.47	23

A/F	Atomization air-to-fuel ratio
P_u	Upstream atomization air pressure
P_t	Throat pressure; i.e., calculated pressure at the air orifice (actually the pressure at the vena contracta point)
ρ_t	Calculated air density at the air orifice
$(1/2\ \rho v^2)_A$	Calculated air blast force per unit area
$(1/2\ \rho v^2)_{F/A}$	Calculated ratio of force per unit area of CWF jet to air blast
MMD	Measured mass median diameter of spray droplets
T_t	Temperature at the air orifice
v_t	Velocity of air at orifice
D	Orifice diameter
A	Orifice area
$\dot{m}_F$	Mass flow rate of CWF
C_D	Measured discharge coefficient of air orifices

The approach taken in the analysis is to compute the three quantities that represent the three conditions necessary for good atomization; namely, A/F ratio, force-per-unit area of the air blast $(1/2\ \rho v^2)_A$, and force-per-unit area of the CWF jets, which then provides the ratio $(1/2\ \rho v^2)_{F/A}$. The quantities are computed for all the data of Table 11, and the values that produce low droplet MMDs are then selected as critical conditions that must be met.

The A/F ratios are obtained from measured CWF flow rates and from measured atomizing air pressures (P_u) and discharge coefficients (C_D) in the normal manner for critical orifice flow as used throughout the study. The MMD values are those measured during testing.

The force per unit area of the atomization air blast and the CWF jets is given by the quantity $1/2\ \rho v^2$ for each stream. The calculation of this value for the CWF jets is straightforward because the flow is incompressible. From the continuity relationship:

$$\dot{m}_F = \rho_F \cdot v_F \cdot A_F$$

With a value of ρ_F taken as 1.17 g/cm^3 and measured A_F and $\dot{m}_F$ data, values of v_F for the CWF jets are calculated and the quantities $(1/2\ \rho v^2)_F$ obtained. Note that $\dot{m}_F$ refers only to the mass flow of one of the two CWF streams of each test.

Estimation of $1/2\ \rho v^2$ values for the air blasts is somewhat more complex because the flow is compressible. The flow in all cases is choked; i.e., the upstream air pressure is at least double the ambient pressure. The approximation is made that gas dynamic conditions at the air orifice correspond to those at the throat of a choked nozzle, and further that the throat conditions do not change appreciably downstream to the collision zone of air and CWF (or that any change is relatively constant from one orifice to another). This approximation seems acceptable for purposes here. In actuality, the gas properties are somewhat different at these two locations because the air blast is expanding, with some decrease in pressure and temperature and a net decrease in density. In addition, it is entraining external air to some extent. The justification for the assumption, however, is based on the fact that these changes are small because the collision zone is barely a few orifice diameters downstream of the "throat" and is even closer to the vena contracta, which is a truer measure of the validity of the assumption. In fact, in photographs, an expansion angle of the air blast is barely detectable. So while the assumption introduces some imprecision into the analysis, it should not seriously affect the overall purpose which is to allow design parameters to be estimated.

The air density at the atomizer throat is given by:

$$\rho_t = P_t M/RT_t$$

where R is the ideal gas constant = 82.05 atm cm^3/°K mole.

From gas dynamics for critical flow:

$$T_t = T_u \left(\frac{2}{\gamma + 1}\right) = 0.833\ T_u$$

$$P_t = P_u \left(\frac{2}{\gamma + 1}\right)^{\frac{\gamma}{\gamma - 1}} = 0.528\ P_u$$

The throat velocity is equal to the velocity of sound of air at the throat temperature:

$$v_t = \sqrt{\frac{\gamma RT_t}{M}} = \sqrt{\frac{1.167\ RT_u}{M}} \text{ cm/sec}$$

where $R = 8.3 \times 10^7$ erg/mole deg. Since air only was employed as the atomizing fluid and choked conditions prevailed in all experiments, v_t is the same for all tests.

Alternatively, v_t may be calculated from $v_t = \dot{m}_A/\rho_t A_t$. The mass flow rate of air is computed as mentioned earlier from:

$$\dot{m}_A = C_D P_u A_A \sqrt{\frac{\gamma M}{RT_u}} \quad (0.58)$$

where the 0.58 factor is given by $\left(\frac{2}{\gamma + 1}\right)^{\frac{\gamma + 1}{2(\gamma - 1)}}$, with γ, the heat capacity ratio, equal to 1.4 for air.

Using these relationships, the values for the quantities of Table 11 were computed. The conditions in the five sets of data of Table 11 that produced efficient atomization were then selected and are collected in Table 12. It is important to note that the conditions that produced the very finest MMDs were not necessarily chosen, but rather conditions that were judged more practical were sometimes taken. For example, at a capacity equivalent to 2.86 MMBTU/H, the conditions listed in Table 12 refer to an MMD of 27 microns. While experimentally, it was found that an MMD as low as 24 microns could be obtained, the A/F ratio necessary to achieve this was 0.64, or 25% higher than the 0.51 value for 27 microns. Even if this difference were "real" and not within experimental error, it would not be worth going to such a much greater A/F for such a small decrease in MMD. At a capacity of 4.3 MMBTU/H, the MMD is an average of the three values obtained at an A/F of 0.39.

Examining the data of Table 12, the following conclusions can be drawn. In order to produce fine droplets, the best conditions are an A/F ratio of about 0.4 or greater; the air blast must have a pressure force given by $1/2\ \rho v^2$ of about 1.7×10^6 dynes/cm^2 or greater; and the force of each CWF

jet must be somewhat greater than that of the air blast in order for those jets to penetrate - i.e., the ratio of 1/2 ρv^2 quantities of CWF to air must be approximately 1.4 or greater.

Table 12. Values Selected from Table 11 for Efficient Atomization Conditions

Capacity (MMBTU/H)	MMD (microns)	A/F	$(1/2\ \rho v^2)_{air} \times 10^6$	$(1/2\ \rho v^2)_{F/A}$
0.24	60	0.24	1.1	0.4
0.40	45	0.3	2.2	0.6
1.1	27	0.54	2.4	1.4
2.86	27	0.51	1.7	1.9
4.3	22	0.39	1.9	1.9
Criteria for Best Atomization		≥ 0.4	≥ 1.7	≥ 1.4

The data of Table 12 are plotted in Figure 9, which shows clearly that the opposed-jet atomizer operates better at larger capacity. Results below 1 MMBTU/H show poorer MMDs, albeit at lower A/F. This is attributable to not being able to achieve a large enough ratio of $(1/2\ \rho v^2)_{F/A}$ at low capacity. Physically, this corresponds to not being able to use an orifice of small enough diameter because of clogging problems. As capacity increases above 1 MMBTU/H, MMD shows a modest decrease, and A/F improves substantially. This trend is predicted to continue at even higher capacity above 4.3 MMBTU/H because the quantity $(1/2\ \rho v^2)_A$ can be increased without encountering any limitations on the requirement to also keep $(1/2\ \rho v^2)_F$ high. Testing in this higher capacity regime could not be conducted because of equipment limitations.

The question could arise whether it would be advantageous to use an atomizing fluid other than air. By combining the previous equations for ρ_t and v_t:

$$(1/2\ \rho v^2)_A = \frac{1}{2} \cdot \frac{P_t M}{RT_t} \cdot \frac{\gamma R T_t}{M} = 1/2\ \gamma P_t$$

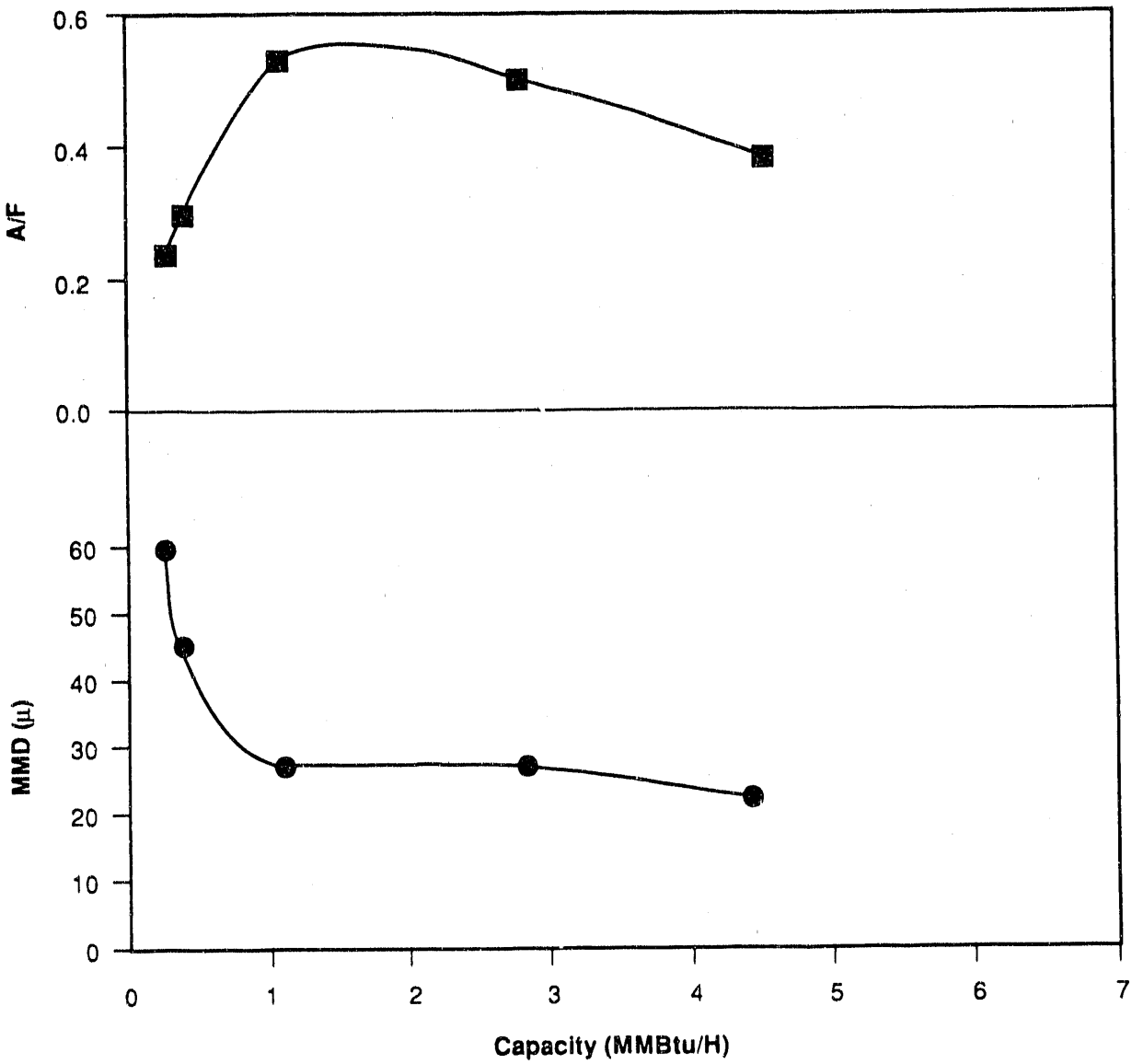

Figure 9

Plot of Data of Table 12 Showing Required A/F and Attained Minimum MMD at Different Atomizer Capacities

This shows that there is only a weak dependence of the force of the atomizing blast on the gas used. Similarily, heating the gas is predicted to have no effect, except in the actual droplet shattering process itself, which is not treated here.

Example Calculation

It is of interest to apply the above procedure to a sample case, chosen here as the PETC atomizer to be operated at 0.5 MMBTU/H on a 57% CWF. The procedure is not to calculate explicitly the atomizer parameters for maximum performance, but rather to develop a table covering a range of each of the parameters and then to select a set of conditions from the tabulation. This is done in Table 13 where the data are based on three CWF orifice diameters of 0.020", 0.018", and 0.015" and three atomizing air orifice diameters of 1/16", 3/32", and 1/8". In addition, three A/F ratios of 0.3, 0.4, and 0.5 are chosen. From the foregoing equation for $\dot{m}_A$, the upstream pressure is calculated:

$$\dot{m}_A = C_D P_u A_A (1.59) (0.58)$$

where P_u here will be in psia when the factor 1.59 is used. Values of $\dot{m}_A$ are obtained from $\dot{m}_F$ and A/F values. A discharge coefficient was measured only for the 1/8" orifice of the PETC atomizer ($C_D = 0.60$) and is taken to be the same for the other assumed orifice sizes. With P_u values, the other quantities in Table 13 are readily calculated as described above.

The conditions to be met for maximum performance are listed in Table 12, and it is seen in Table 13 that the only sets of parameters that meet these conditions are a 3/32" atomizing air orifice operated on upstream pressure of 68.5 psia or greater, with CWF orifices of 0.015" diameter. The problem achieving these conditions is that a 0.015" orifice would likely plug with CWF inasmuch as a 0.012" CWF orifice plugged almost immediately in repeated tests. An 0.018" CWF orifice did perform without plugging; however, even this size would not meet the conditions for maximum performance. A 0.020" orifice was chosen in order to provide margin for plugging even though some spray droplet size would have to be sacrificed. Either a 3/32" or 1/8"

Table 13. Tabulation of Data for a Range of Parameters for the PETC Atomizer

Capacity: 0.50 MMBTU/H; $\dot{m}_F$ = 7.3 g/sec total; 3.65 g/sec per orifice

D_F (inch)	A_F (cm^2)	v_F (cm/sec)	$(1/2\ \rho v^2)_F$ ($dyne/cm^2$)
0.020	2.03×10^{-3}	1537	1.38×10^6
0.018	1.64×10^{-3}	1898	2.11×10^6
0.015	1.14×10^{-3}	2732	4.37×10^6

D_A (inch)	A_A (cm^2)	A/F	$\dot{m}_A$ (g/sec)	P_u (psia)	$\rho_t \times 10^{-3}$ (g/cm^3)	$(1/2\ \rho v^2)_A \times 10^6$ ($dyne/cm^2$)	$\frac{(1/2\ \rho v^2)_{F/A}}{D_F}$ 0.020"	0.018"	0.015"
1/16	0.0198	0.3	2.19	115	5.84	2.93	0.47	0.72	1.49
		0.4	2.92	154	7.82	3.92	0.35	0.53	1.11
		0.5	3.65	192	9.74	4.88	0.28	0.43	0.89
3/32	0.0445	0.3	2.19	51.3	2.60	1.30	1.06	1.61	3.35
		0.4	2.92	68.4	3.47	1.74	0.79	1.21	2.50
		0.5	3.65	85.4	4.33	2.17	0.64	0.98	2.03
1/8	0.0792	0.3	2.19	28.8	1.46	0.73	1.89	2.98	5.98
		0.4	2.92	38.4	1.95	0.98	1.41	2.15	4.46
		0.5	3.65	48.0	2.44	1.22	1.13	1.72	3.58

air orifice can be chosen. The former provides a stronger air blast for better atomization, but the strength of the fuel jets (0.79) is relatively weaker and will not penetrate the air stream so well. The 1/8" air orifice provides a relatively weaker air blast (0.98), but the fuel jets will penetrate adequately.

5.0 CONCLUSIONS AND RECOMMENDATIONS

The present program represented Phase II of a study to evaluate a new concept in atomization. In Phase I of the work, which ended in 1989, the basic validity of this opposed-jet atomization process was established in both cold-flow and combustion testing. In this second phase, which involved cold-flow testing only, a broader evaluation of the performance of the atomizer was undertaken. A considerable number of individual tasks were performed, and among the most significant results of the study were those that related to testing at lower and higher capacity. When the prototype test unit was scaled down to about one quarter of the capacity of 1 MMBTU/H, the nominal capacity of Phase I, performance declined as measured by spray droplet size. As the unit was scaled up to 4.3 MMBTU/H, performance improved significantly. Based on the data extending over an order of magnitude in capacity, an analysis of the atomization process was performed. In this modeling effort, it was shown that there are three conditions necessary for maximum performance: (1) the atomizing air-to-fuel ratio must be about 0.4 or greater; (2) the force of the atomizing air blast must be sufficient to shatter CWF into fine droplets (the value of this force was found to be approximately $\geq 1.7 \times 10^6$ dyne/cm^2 based on the modeling approach); and (3) the force of the CWF jets must be sufficient to allow the fuel to penetrate into the air stream (this is expressed as a ratio of force of CWF jets to air blast, with a value of ≥ 1.4).

Future work related to the opposed-jet atomizer should focus on three areas: (1) reducing the atomizing air-to-fuel ratio to ≤ 0.2; (2) investigating scaleup to capacities greater than 4.3 MMBTU/H; and (3) solving any problems that might be uncovered during combustion testing, such as buildup of CWF on the atomizer face from the spray in the furnace.

APPENDIX A

Comparison of Sauter Mean Diameter (SMD) and Mass Median Diameter (MMD) for CWF Spray Droplets

The MMD of a collection of particles or droplets represents the size above and below which lies 50% of the mass of the group. The SMD is defined as the diameter of a particle or drop having the same surface-area-to-volume ratio as the group or spray. As the average diameter of a collection increases, the SMD increases and the average surface-area-to-volume ratio decreases. The SMD is often used in connection with atomization processes because it is thought to better characterize a spray. Six sets of data are collected below (selected at random) from measurements of CWF sprays obtained in Phase I and II of the atomization study. The MMD and the SMD for each spray were calculated and are shown for comparison.

Sauter Mean Diameter is defined as:

$$SMD = d_{32} = \left[\frac{\sum X_i d_i^3}{\sum X_i d_i^2}\right] \qquad (1)$$

where X_i is the number of particles in a size range (a cell or bin or cut) of a spray and d_i is the average diameter in that size range. The summation is taken over the whole range of droplet sizes. Since the Malvern particle size analyzer used in obtaining the data below yields the weight fraction W_i in each size range rather than the number of particles, the above expression is rewritten as:

$$SMD = \frac{\dfrac{W_i d_i^3}{\rho \frac{\pi}{6} d_i^3} + \ldots}{\dfrac{W_i d_i^2}{\rho \frac{\pi}{6} d_i^3} + \ldots}$$

$$SMD = \frac{W_1 + W_2 + \ldots}{\dfrac{W_1}{d_1} + \dfrac{W_2}{d_2} + \ldots}$$

The calculated SMD and MMD values are:

CWF Spray	MMD (microns)	SMD (microns)
A	20	15
B	19	14
C	22	15
D	25	15
E	19	12
F	25	17

The average ratio of SMD to MMD of these data is 0.68. If data are reported as SMD rather than MMD, the values will generally be lower.

Malvern Particle Size Data for Six CWF Sprays

d_i	A (W_i)	B (W_i)	C (W_i)	D (W_i)	E (W_i)	F (W_i)
74.5	-	-	-	7.7	-	-
57.4	-	-	-	7.7	5.6	3.9
44.6	-	-	-	12.1	9.7	22.4
34.7	17.4	4.3	14.1	11.7	8.4	10.5
27.0	21.2	34.3	28.7	12.3	14.2	19.8
21.1	3.2	5.8	8.3	14.8	13.7	19.3
16.5	18.9	15.3	14.3	8.7	10.7	8.0
13.0	16.5	21.8	14.6	6.0	8.8	2.6
10.3	10.7	7.1	9.1	5.6	8.9	5.7
8.2	6.9	5.9	5.3	3.6	6.8	3.2
6.5	3.6	2.6	3.0	3.4	5.6	2.5
2.9	1.6	2.8	2.5	6.3	7.5	4.1

APPENDIX B

DRAWINGS OF PETC ATOMIZER

B-2

NOTES:

1. ITEMS 7 & 9 ARE MANUFACTURED BY
   CAJON CO.
   9760 SHEPARD RD.
   MACEDONIA, OH 44056

2. ITEMS 9 & 10 ARE MANUFACTURED BY
   SWAGELOCK CO.
   SOLON, OH 44139

3. ITEMS 14 & 15 ARE MANUFACTURED BY
   PARKER SEAL
   O-RING DIV
   2360 PALUMBO DR
   P.O. BOX 11751
   LEXINGTON, KY 40512

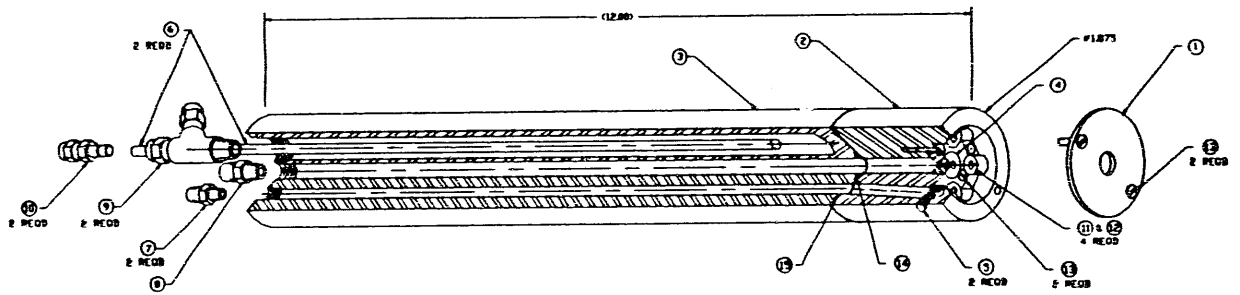

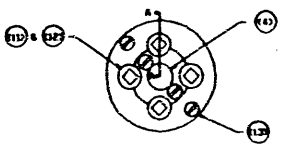

CAP FACE

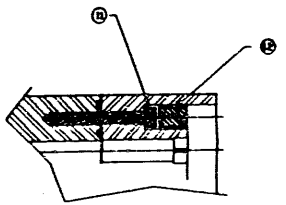

Section A-A

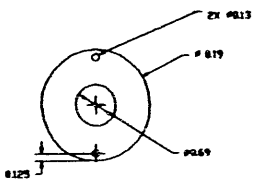

ALUMINUM PLATE

QTY ITEM	PART OR IDENTIFYING NO.	ITEM NO	DESCRIPTION	REF SPEC	REMARKS
1	2-029	15	VITON O-RING, V884-75		SEE NOTE 3
1	2-015	14	VITON O-RING, V884-75		SEE NOTE 3
4	5-40UNC	13	SLOTTED PAN HEAD SCREW	2A	.75 LG.
4	1/8-NPT	12	HEX HEAD PIPE SCREW		.75 LG.
4	10-24UNRC	11	HEX HEAD SCREW	2A	1.50 LG.
2	B-400-R-3 -BT	10	REDUCER		SEE NOTE 2
2	B-810-3TMT	9	MALE RUN TEE		SEE NOTE 2
1	B-4-HRN-2	8	HEX REDUCING NIPPLE		SEE NOTE 1
2	B-2-HRN-1	7	HEX REDUCING NIPPLE		SEE NOTE 1
2	NALGENE689	6	POLYPROPYLENE TUBING		15.0 LG.
2		5	ORIFICE, SLURRY		
1		4	ORIFICE, AIR		
1		3	ATOMIZER SHAFT		
1		2	ATOMIZER CAP		
1		1	PLATE, AL ALLOY 6061		0.063 THK.

LIST OF MATERIALS OF THIS UNIT

UNLESS OTHERWISE SPECIFIED
DIMENSIONS ARE IN INCHES
TOLERANCES: ANGLES ±0.5
FRACTIONS ±1/64
2 PLACE DECIMALS ±.01
3 PLACE DECIMALS ±.005
SURFACE ROUGHNESS 125
DO NOT SCALE DRAWING
MATERIAL
SEE PARTS LIST

APPROVALS	BY	DATE
DRAWN	K.MEREDITH	2/13/91
CHECKED	M.HASTINGS	2/13/91
ENGR	K.MEREDITH	2/13/91
PROJ ENG	M.HEATON	2/13/91

APPROVED FOR ARC
HARLEY HEATON

ARC ATLANTIC RESEARCH CORPORATION
VIRGINIA PROPULSION DIVISION
GAINESVILLE, VIRGINIA

COAL WATER FUEL ATOMIZER ASSEMBLY

D

SCALE 1/1 SHEET 1 OF 1

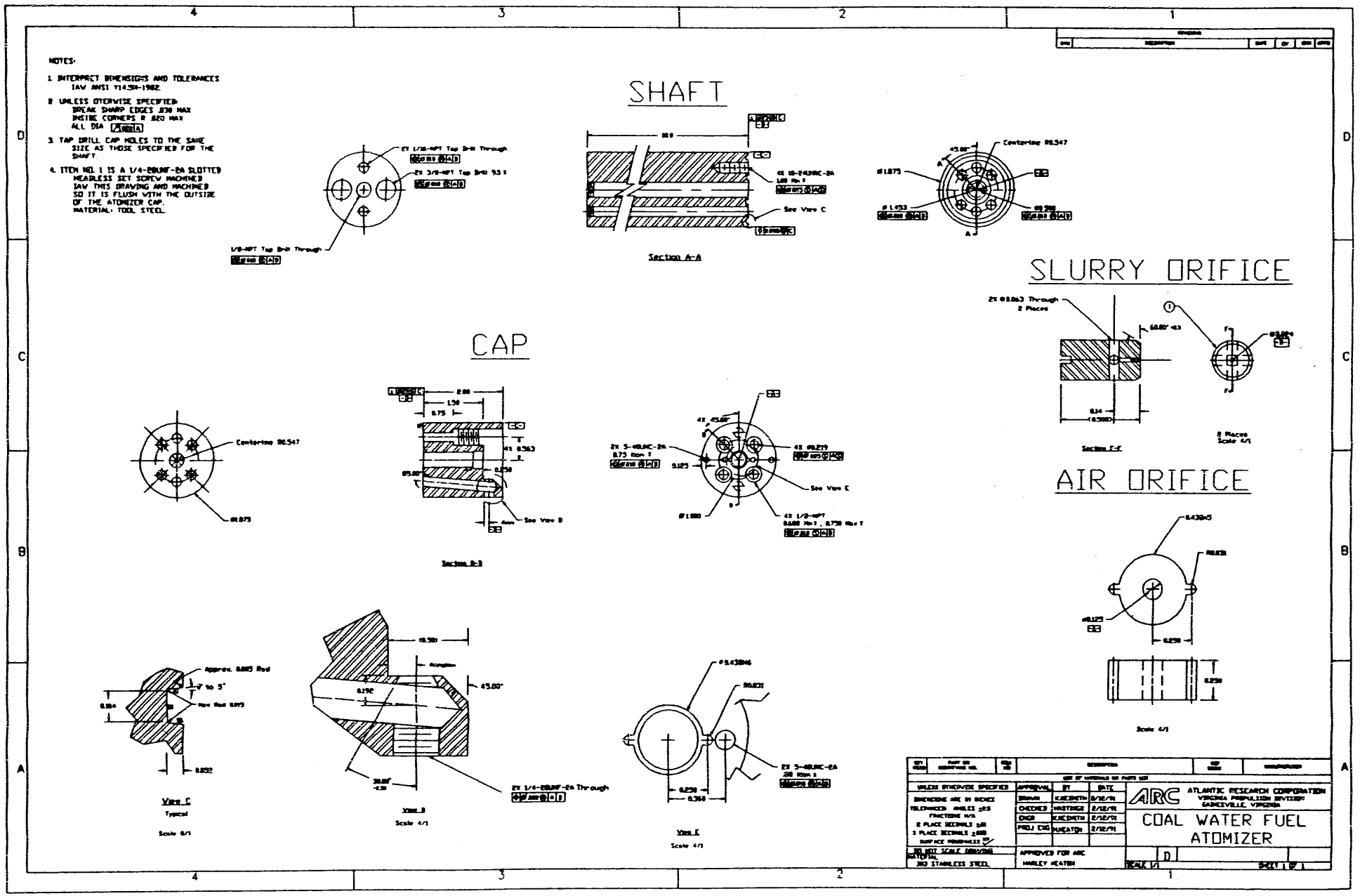
NOTES:
1. INTERPRET DIMENSIONS AND TOLERANCES IAW ANSI Y14.5M-1982.
2. UNLESS OTHERWISE SPECIFIED: BREAK SHARP EDGES .030 MAX INSIDE CORNERS R .020 MAX ALL DIA
3. TAP DRILL CAP HOLES TO THE SAME SIZE AS THOSE SPECIFIED FOR THE SHAFT.
4. ITEM NO. 1 IS A 1/4-28UNF-2A SLOTTED HEADLESS SET SCREW MACHINED IAW THIS DRAWING AND MACHINED SO IT IS FLUSH WITH THE OUTSIDE OF THE ATOMIZER CAP.
MATERIAL: TOOL STEEL
SHAFT
Section A-A
CAP
SLURRY ORIFICE
AIR ORIFICE
View C
Typical
View B
View E
COAL WATER FUEL ATOMIZER
ATLANTIC RESEARCH CORPORATION
APPROVED FOR ARC
HARLEY HEATON
303 STAINLESS STEEL

APPENDIX C

D_{80}, D_{50}, and D_{20} Values Measured with the PETC Unit (See Table 6)

Test Series 1	D_{80}	D_{50}	D_{20}
	81, 75	47, 46	29, 28
	61, 61	40, 40	21, 21
	59, 59	39, 38	19, 18
	60, 56	37, 36	17, 16

Test Series 2	D_{80}	D_{50}	D_{20}
	199	61	25
	75	42	18
	78	37	16
	68, 44	30, 21	13, 10

Test Series 3	D_{80}	D_{50}	D_{20}
	564	38	17
	52	26	13
	39	22	11
	37	20	10

Test Series 4	D_{80}	D_{50}	D_{20}
	134	50	18
	107	42	15
	105	41	13
	100	38	13

Test Series 5

D_{80}	D_{50}	D_{20}
79	32	16
48	26	13
46	23	11
61	28	11

Test Series 6

D_{80}	D_{50}	D_{20}
107	48	20
94	41	16
93	41	14
84	40	13

Test Series 7

D_{80}	D_{50}	D_{20}
119, 107	54, 50	22, 21
108, 108	47, 46	18, 18
91, 86	40, 39	16, 20
80, 84	35, 37	14, 15

Test Series 8

D_{80}	D_{50}	D_{20}
47, 45	26, 25	14, 14
39, 37	22, 21	12, 11
38, 38	21, 22	12, 11
37, 35	20, 20	11, 10

END

DATE
FILMED
8/20/92